



저작자표시-비영리-변경금지 2.0 대한민국

이용자는 아래의 조건을 따르는 경우에 한하여 자유롭게

- 이 저작물을 복제, 배포, 전송, 전시, 공연 및 방송할 수 있습니다.

다음과 같은 조건을 따라야 합니다:



저작자표시. 귀하는 원저작자를 표시하여야 합니다.



비영리. 귀하는 이 저작물을 영리 목적으로 이용할 수 없습니다.



변경금지. 귀하는 이 저작물을 개작, 변형 또는 가공할 수 없습니다.

- 귀하는, 이 저작물의 재이용이나 배포의 경우, 이 저작물에 적용된 이용허락조건을 명확하게 나타내어야 합니다.
- 저작권자로부터 별도의 허가를 받으면 이러한 조건들은 적용되지 않습니다.

저작권법에 따른 이용자의 권리는 위의 내용에 의하여 영향을 받지 않습니다.

이것은 [이용허락규약\(Legal Code\)](#)을 이해하기 쉽게 요약한 것입니다.

[Disclaimer](#)

工學博士 學位論文

**Application and Characterization of
Pyrrolinium-based Ionic liquids as
Electrolytes for Lithium Ion
Batteries**

리튬이차전지 전해질용
피롤리늄계 이온성 액체의
성능평가 및 적용

2017年 8月

서울대학교 大學院

化學生物工學部

金 亨 泰

Application and Characterization of Pyrrolinium-based Ionic liquids as Electrolytes for Lithium Ion Batteries

指導教授：金 榮 奎

이 論文을 工學博士 學位論文으로 提出함

2017年 2月

서울大學校 大學院

化學生物工學部

金 亨 泰

金 亨 泰 의 工學博士 學位論文을 認准함

2016年 12月

委 員 長 _____ (印)

副委員長 _____ (印)

委 員 _____ (印)

委 員 _____ (印)

委 員 _____ (印)

**Application and Characterization of
Pyrrolinium-based Ionic liquids as
Electrolytes for Lithium Ion
Batteries**

A THESIS SUBMITTED IN PARTIAL FULFILLMENT OF
THE REQUIREMENTS FOR THE DEGREE OF DOCTOR
OF PHILOSOPHY IN ENGINEERING AT THE
GRADUATED SCHOOL OF SEOUL NATIONAL
UNIVERSITY

August 2017

by

Hyung-Tae Kim

Supervisor

Young Gyu Kim

ABSTRACT

Lithium ion batteries (LIBs) have been used as a battery of portable electronic device and concerned as a one of the most promising energy conversion/storage systems for large-scale devices such as electric vehicles (EVs) and energy storage systems (ESSs). However, the need for the high energy density of current LIBs have been increased, which results that many research have been focus on the advanced electrode materials for high working voltage, a large specific capacity to enhance overall energy density of the lithium ion cells. In other words, the relatively low safety of current organic electrolyte should be overcome to catch up with the enhancement of the energy density for reaching the high level of LIBs. For increasing the safety performance of the conventional electrolyte, many attempts have been studied to apply ionic liquids as alternative electrolyte or additive.

Ionic liquids are ionic species that remain in liquid phase at room temperature even if they are composed of ionic species, cations and

anions. Due to ionic interaction, they have unique properties such as high ionic conductivity, non-volatility, and non-flammability as well as a wide liquid range and wide electrochemical stability window. In spite of these advantages, the ILs are not useful as electrolytes for LIBs owing to somewhat defect such as decomposition or high viscosity. As already reported, the well-known ILs such as imidazolium-based ILs have been investigated to allow them apply the LIBs, which is not carried on its acidic proton of C-2 position in imidazolium structure. To exclude the active proton, pyrrolidinium and piperidinium-based ILs have been researched; however, their relatively high viscosity is the obstacle to facilitate in LIBs. To enhance both the mobility of Li^+ and the safety performance of LIBs, we suggest the pyrrolinium-based ILs with multifunctional groups such as a planar sp^2 carbon of C=N double bond, a C-O ether linkage, and no unstable C-H bond, which would be beneficial to improve the physical properties as well as electrochemical performances. Among the prepared pyrrolinium-based ILs, the *N*-ethyl-2-methoxypyrrolinium bis(fluorosulfonyl)imide (E(OMe)PyrI-FSI)

exhibit the highest value of ionic conductivity, and the *N*-allyl-2-methoxypyrrolinium bis(fluorosulfonyl)imide (A(OMe)Pyr1-FSI) shows the best electrochemically performance and lithium ion mobility.

To obtain the synergetic effect of pyrrolinium-based ILs and carbonate solution, we prepared the binary electrolytes systems composed of two type electrolytes. Among the prepared pyrrolinium-based ILs, the E(OMe)Pyr1-FSI is chosen as the one of the binary electrolytes systems due to its highest value of ionic conductivity. In ionic conductivity of these binary electrolytes, the optimum compositions are 40 wt% and 60 wt% of pyrrolinium-based ILs. Additionally, when the 60 wt% of E(OMe)Pyr1-FSI (E60) is in binary system, the SET (self extinguish time, s g⁻¹) is outstandingly reduced. In electrochemical performance, all of the binary electrolytes exhibit the similar results that of the conventional carbonate. It should be noted that the E 60 binary system is the best synergetic effect on both the electrochemical performance and fire-retarding characteristic.

Keywords : Lithium ion battery, pyrrolinium-based ionic liquids, FSI anion, thermal stability, binary electrolytes

Student number : 2009-20986

TABLE OF CONTENTS

ABSTRACT	i
LIST OF FIGURES	x
LIST OF TABLE	xiii
LIST OF SCHEMES	xv
LIST OF ABBREVIATIONS	xvi
Introduction	1
1. 1. Lithium Ion Batteries	1
1.1. Introduction of lithium ion batteries	1
1.2. Safety issue of LIBs	2
2. Ionic Liquids	6
2.1. Introduction of ionic liquids.....	6
2.2. Species of ionic liquids.....	7
2.3 Application of ionic liquids.....	10

2.3.1 Reaction solvent in organic synthesis	10
2.3.2 Lubricants.....	14
2.3.3 Electrolytes for LIBs.....	15
Results and discussion	19
1. Synthesis and Properties of <i>N</i>-alkyl-2-methoxypyrrolinium	
 bis(fluorosulfonyl)imide	19
1.1. Strategy	19
1.2. Preparation.....	24
1.3. Thermal behaviors.....	26
1.4. Physical properties.....	29
1.5. Electrochemical stability	31
1.6. Electrochemical performance	34

1.7. Summary	42
2. Preparation and Properties of Binary Electrolytes	44
2.1. Strategy	44
2.2. Preparation	46
2.3. Flammability test	47
2.4. Physical properties	51
2.5. Electrochemical stability	54
2.6. Electrochemical performance	57
2.7. Summary	63
Conclusions.....	66
Experimental Details.....	69

1. General	69
2. General Procedure for the Preparation of the Pyrrolinium-based Ionic Liquids	72
2.1. General procedure for the preparation of <i>N</i> -alkyl-2-pyrrolidinone	72
2.2. General procedure for the preparation of <i>N</i> -alkyl-2-methoxypyrrolinium methyl sulfates	73
2.3. General procedure for the anion metathesis - Preparation of <i>N</i> -alkyl-2-methoxypyrrolinium bis(fluorosulfonyl)imides	75
2.4. Preparation of the binary electrolytes of E(OMe)Pyr1-FSI.....	77
3. Electrochemical Performance	77
3.1. Preparation of electrode and cell fabrication	77
3.2. Electrochemical characterization	78
REFERENCES	80
APPENDICES	84

ABSTRACT IN KOREAN.....105

LIST OF FIGURES

Figure 1. Schematics of Lithium ion battery	3
Figure 2. Various species of ionic liquids	9
Figure 3. Wittig reaction in BMIm-PF ₆	12
Figure 4. Suzuki coupling in BMIm-BF ₄	13
Figure 5. Diels-Alder reaction in BMIm-BF ₄	14
Figure 6. Molecular structure of IL lubricants	15
Figure 7. Rate properties of various imidazolium-based ILs	17
Figure 8. Electrochemical windows of piperinium-based ILs	21
Figure 9. Electrochemical windows of pyrrolidinium-based ILs	21
Figure 10. Outline of the novel strategy; pyrrolinium-based ionic liquids with methoxy substituent	22
Figure 11. Cathodic limit of 6 different electrolytes.....	32
Figure 12. Anodic limit of 6 different electrolytes	32
Figure 13. Cycle performance of the LiFePO ₄ /Li ⁺ cells in six different electrolytes at 25 °C.....	36
Figure 14. Potential profiles of the LiFePO ₄ /Li ⁺ cell in six different electrolytes at 25 °C at the 1 st cycle	36
Figure 15. Potential profiles of the LiFePO ₄ /Li ⁺ cell in six different electrolytes at 25 °C at the 50 th cycle	37
Figure 16. Rate performance of the LiFePO ₄ /Li ⁺ cell in six different	

electrolytes at 25 °C	37
Figure 17. Potential profile of rate performance of the LiFePO ₄ /Li ⁺ cell in E(OMe)Pyr1-FSI electrolytes at 25 °C from 0.1 C to 5 C	39
Figure 18. Potential profile of rate performance of the LiFePO ₄ /Li ⁺ cell in P(OMe)Pyr1-FSI electrolytes at 25 °C from 0.1 C to 5 C	39
Figure 19. Potential profile of rate performance of the LiFePO ₄ /Li ⁺ cell in A(OMe)Pyr1-FSI electrolytes at 25 °C from 0.1 C to 5 C	40
Figure 20. Potential profile of rate performance of the LiFePO ₄ /Li ⁺ cell in PMPyrd-FSI electrolytes at 25 °C from 0.1 C to 5 C	40
Figure 21. Potential profile of rate performance of the LiFePO ₄ /Li ⁺ cell in EMIm-FSI electrolytes at 25 °C from 0.1 C to 5 C	41
Figure 22. Potential profile of rate performance of the LiFePO ₄ /Li ⁺ cell in carbonate electrolytes at 25 °C from 0.1 C to 5 C	41
Figure 23. Outline of the binary electrolytes between the carbonate and the pyrrolinium-based ionic liquids	44
Figure 24. Images of the flammability tests of E 00, E 20, E 40, E 60, E 80, E 100 for direct flame combustion test	47
Figure 25. Images of the flammability tests of E 00, E 20, E 40, E 60, E 80, E 100 for indirect flame combustion test	48
Figure 26. Viscosity of the binary electrolytes at 25 °C (blue) and 60 °C (red).....	51

Figure 27. Ionic conductivity of the binary electrolytes at 25 °C (blue) and 60 °C (red)	52
Figure 28. Cathodic limit of 6 different electrolytes	54
Figure 29. Anodic limit of 6 different electrolytes.....	55
Figure 30. Cycle performance of the LiFePO ₄ /Li ⁺ cells in six different electrolytes at 25 °C	57
Figure 31. Cycle performance of the LiFePO ₄ /Li ⁺ cells in eight different electrolytes at 60 °C	58
Figure 32. Potential profiles of the LiFePO ₄ /Li ⁺ cell in five different electrolytes at 60 °C at 1 st cycle	59
Figure 33. Potential profiles of the LiFePO ₄ /Li ⁺ cell in five different electrolytes at 60 °C at 50 th cycle	60
Figure 34. SEM images of the LiFePO ₄ cathode in each binary electrolyte after the 50 th cycle between 2.5 and 3.9 V (vs Li/Li ⁺) at 60 °C	61

LIST OF TABLES

Table 1. Physical properties of FSI anion based ILs	18
Table 2. Physical properties of pyrrolidinium and piperidinium ionic liquids.....	20
Table 3. Preparation of <i>N</i> -alkyl-2-methoxypyrrolinium bis(fluorosulfonyl)imide	26
Table 4. Thermal behaviors of pyrrolinium-based FSI ionic liquids.....	27
Table 5. Physical properties of pyrrolinium FSI ionic liquids	30
Table 6. Physical properties of pyrrolinium FSI ionic liquids with 1.0 M lithium salt.....	31
Table 7. Initial Discharge Capacity and Retention ratio of six different electrolytes at 25 °C	35
Table 8. Lithium ion transference number of six different electrolytes at 25 °C	42
Table 9. Flammability Tests (Direct and Indirect Flame) and SET Values.....	50
Table 10. Physical properties of binary electrolytes and ILs with 1.0 M lithium salt.....	53

Table 11. Initial Discharge Capacity and Retention ratio of six different electrolytes at 25 °C	62
Table 12. Initial Discharge Capacity and Retention ratio of six different electrolytes at 60 °C.....	63

LIST OF SCHEMES

Scheme 1. Synthesis of <i>N</i> -alkyl-2-methoxypyrrolinium bis(fluorosulfonyl)imide and abbreviation of the ILs used in this study	25
---	----

LIST OF ABBREVIATIONS

M(OMe)Pyr1	1-methyl-2-methoxy-pyrrolinium
E(OMe)Pyr1	1-ethyl-2-methoxy-pyrrolinium
P(OMe)Pyr1	1-propyl-2-methoxy-pyrrolinium
A(OMe)Pyr1	1-allyl-2-methoxy-pyrrolinium
PMPyrr	Propylmethylpyrrolidinium
AMPyrr	Allylmethylpyrrolidinium
AAPyrr	Diallylpyrrolidinium
PMPip	Propylmethylpiperidinium
AMPip	Allylmethylpiperidinium
AAPip	Diallylpiperidinium
CV	cyclic voltammetry
δ	chemical shift
D	Doublet
Dd	doublet of doublet
DMC	dimethyl carbonate
DSC	differential scanning calorimetry
η	Viscosity
EC	ethylene carbonate
EMC	ethyl methyl carbonate
EMIm	1-ethyl-3-methylimidazolium

EW	electrochemical window
Fc	ferrocene
FSI	bsi(fluorosulfonyl)imide
h	hour(s)
Hz	hertz
IL	ionic liquid
<i>J</i>	coupling constant(s)
LIB	lithium ion battery
LSV	linear sweep voltammetry
M	mole(s) per liter
m	multiplet
ND	not detected
NMR	nuclear magnetic resonance spectroscopy
PC	propylene carbonate
PMPyrd	propylmethylpyrrolidinium
q	quartet
quant.	quantitative
RT	room temperature
RTIL	room temperature ionic liquid
σ	ionic conductivity
s	singlet

SEI	solid electrolyte interphase
sext	Sextet
T	Temperature
<i>t</i>	Time
t	Triplet
T_c	crystallization temperature
T_d	decomposition temperature
TFSI	bis(trifluoromethanesulfonyl)imide
TGA	thermogravimetric analysis
T_m	melting point
VC	vinyl carbonate
SET	self extinguish time

Introduction

1. Lithium Ion Batteries

1.1 Introduction of lithium ion batteries

In recent years, there are many attempts to develop smart grids functionalized in energy storage devices of renewable energy and electric vehicles. Lithium ion batteries (LIBs) have been considered as one of the most promising energy conversion/storage systems due to their long-life cycling time and reasonable rate performance.¹⁻²

Initially, lithium has long received much attention as a promising anode material. The interest in this alkali metal has arisen from the combination of its two unique properties:

- (1) lithium metal is the most electronegative metal
- (2) lithium metal is the lightest metal (0.534 g cm^{-3}).

In the 1950s lithium metal as anode material was found to be stable in a number of non-aqueous solvents despite its reactivity, and the stabilization of anode was attributed to the formation of a protective film on the lithium surface, which prevents it from having a sustained reaction with electrolytes. But, a serious hazard could be caused by

such "dead lithium" crystals, which are electrochemically inactive but chemically hyper-reactive due to their high surface area. When dendrite growth pierces the separator and leading to an internal short, thermal runaway and explosion ensue.^{1,2}

Owing to the dendrite formation, the failure of lithium as an anode prompted the search for a way to circumvent the drastic morphological change of the anode during cell cycling. As a result, host-guest concept was considered, known as intercalation or insertion type electrodes. In 1990 both Sony and Moli noticed the commercialization of cells based on petroleum coke and LiCoO_2 , and in the same year, Dahn and co-workers published their report on the principle of lithium intercalation chemistry with graphitic anodes and the effect of electrolyte solvent in the process.¹⁻³ Obviously, the solid electrolyte interface (SEI) in LIBs graphite anode plays a critical role in enabling a lithium ion device to work reversibly. After that, LIBs have been continuously investigated and developed until commercial lithium-ion batteries were first released and they still have been widely researched.

1.2 Safety issue of LIBs

Nowadays, as the demand for portable electrical devices is rapidly

increased, LIBs have been the one of the most popular types of rechargeable batteries for portable electronics. LIBs are basically composed of four components, which are a positive electrode, a

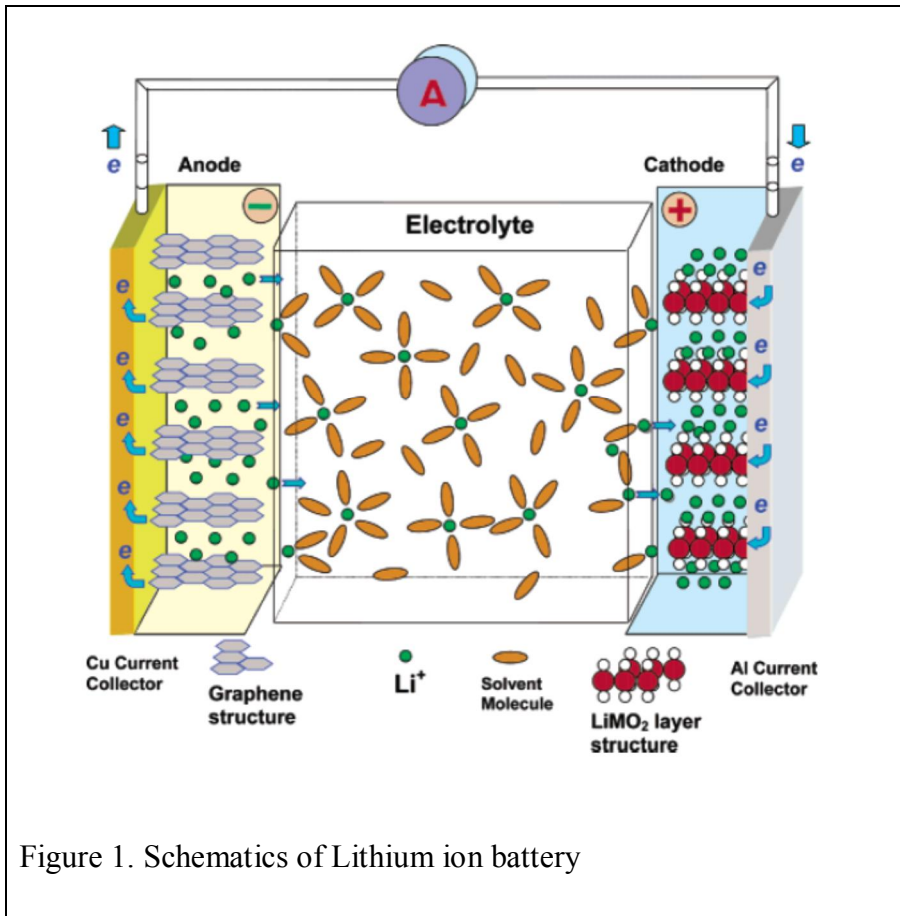


Figure 1. Schematics of Lithium ion battery

negative electrode, a separator, and an electrolyte depicted in Figure 1. LIBs are operated by releasing lithium ions from cathode materials including LiCoO₄, LiFePO₄, to layered carbonaceous anode via electrolytes when it discharging, likewise charging process is performed in reverse. Therefore, stable charge-discharge process of

LIBs by forming the SEI is powerful advantage in rechargeable batteries, which makes the batteries possible to use several times using the principle.³ On the basis of the fundamental principle, LIBs are performed with excellent cycle life and can store more energy per volume than any other types of portable rechargeable battery. In addition, it exhibit higher power, higher energy density, and better charge efficiency than Ni-Cd and nickel metal hydride (NiMH) batteries.

In spite of these advantages, there are still apparent safety issues which result in the explosion caused by flammable and combustible organic solvents in LIBs. Conventional electrolytes in LIBs are composed of cyclic carbonate such as ethylene carbonate (EC), propylene carbonate (PC) and acyclic carbonate including dimethyl carbonate (DMC), ethylmethyl carbonate (EMC), and these carbonate having volatility and flammability are easily exploded by battery ignition from the spark. When the battery ignition occurs, the volatile organic carbonate spontaneously plays a role as a fuel, which means that this situation could generate dangerous thermal runaway.

In the light of safety standpoint, ILs are able to be alternative candidate as the promising electrolyte of LIBs due to non-flammable and non-volatility owing to its unique chemical nature. Additionally, there have been many researches to investigate ILs as an alternative

material for electrolyte in LIBs, as they show the virtue of wide liquid range, high thermal as well as electrical stability, and moderate ionic conductivity.

2. Ionic Liquids

2.1 Introduction of ionic liquids

Organic compound with the strong ionic interaction between the cation and anion have a high melting point in common. However, some ionic compounds have a wide liquid range including room temperature and remain the liquid phase in low temperature area. These ionic species that allow compounds to be in liquid state are called room temperature ionic liquids, frequently abbreviated RTILs or ILs.

Although the ILs are liquids, they have different behaviors comparing to other organic solvents, since they are composed of cation and anion. Firstly, their vapor pressure is negligible and non-volatility allows them to be non-flammable. Additionally, they have known as a wide liquid range, designability as well as good thermal and electrochemical stability.

In this regard, the ILs have been attracted as an alternative material in organic synthesis, lubricants, and electrochemistry in spite of their relatively high viscosity. Besides, non-volatility and non-flammability are noticeable properties, which are the requirements of LIBs demand

and next-generation batteries such as Li-S battery or Li-Air battery.

2.2 Species of ionic liquids

In the beginning, some types of chloride salt with AlCl_3 exhibit a low melting point below room temperature, however, it was too difficult to control the chloride salt due to their easily decomposition under air or water. However, ILs have gotten a lot of attentions since Wilkes synthesized air and water stable ILs with tetrafluoroborate anion in 1992. Since stable ILs is invented, the application of ILs has been accelerated by a lot of researchers.⁴

The cation of ILs are two types; cyclic or acyclic. For example, the cyclic cation having nitrogen atom is imidazolium, pyrrolidinium, pyridinium, pyrimidinium, etc (Figure 2). Already reported⁵, the imidazolium and pyrrolidinium cation structure have been investigated by a lot of researchers due to their thermal stability, low viscosity, and high ionic conductivity. However, in case of the imidazolium cation, the structure has critical defects, which is easily decomposed, particularly under cathodic limit. The decomposition of the imidazolium is affected by the acidic proton at C-2 position in imidazolium ring, which result in the electrochemically unstable characteristic. Thus, many researchers have paid attention to improve

the cathodic stability of cation structures and one of them is the pyrrolidinium or piperidinium ring as a cation of ILs due to their no acidic proton in cation structure. Although these cyclic ring as a cationic species of ILs results in the enhancement of electrochemical stability, their high viscosity and low ionic conductivity have been still investigated to apply the practical LIBs. In this trend, the pyrrolinium ring structure is more planar than pyrrolidinium or piperidinium due to introducing the sp^2 carbon of double bond in cation ring.

In case of anion, it plays a significant role in determining its physical properties. Among various anion candidates, fluorinated anions are generally used due to the dispersion of the anionic character of ILs, which lead to weaken the overall ionic interaction. The development of novel anions and modification studies are active.

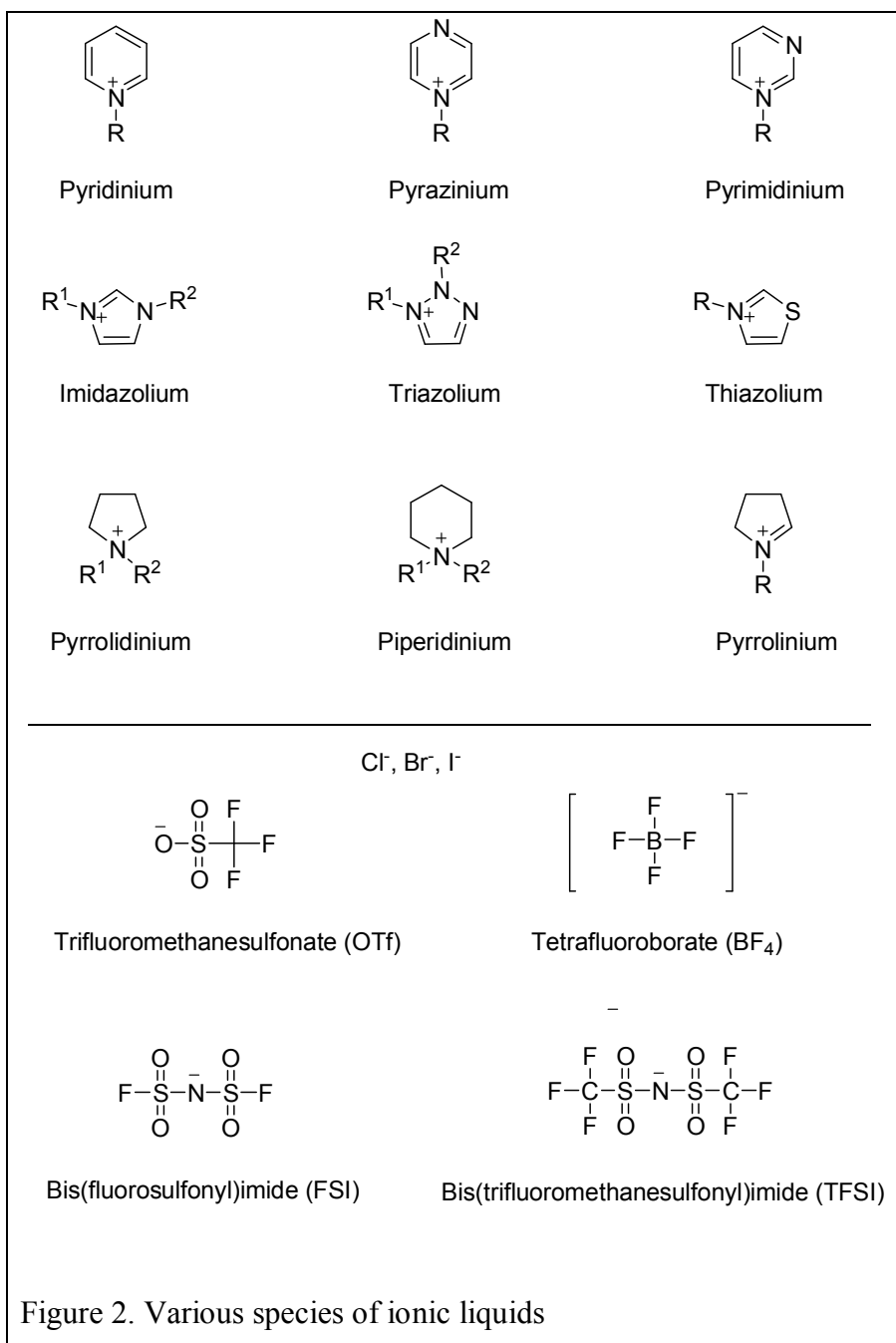


Figure 2. Various species of ionic liquids

2.3 Application of ionic liquids

2.3.1 Reaction solvent in organic synthesis

Recently, ionic liquids are attracting a great deal of attention as possible replacement for conventional molecular solvents for organic reactions. The organic solvents in reaction are dangerous and toxic due to their volatility. Viewed from safety standard, the ILs are good candidate as a green solvent owing to their non-volatility. Besides the non-volatility, a summary of their unique properties in nature is given below.

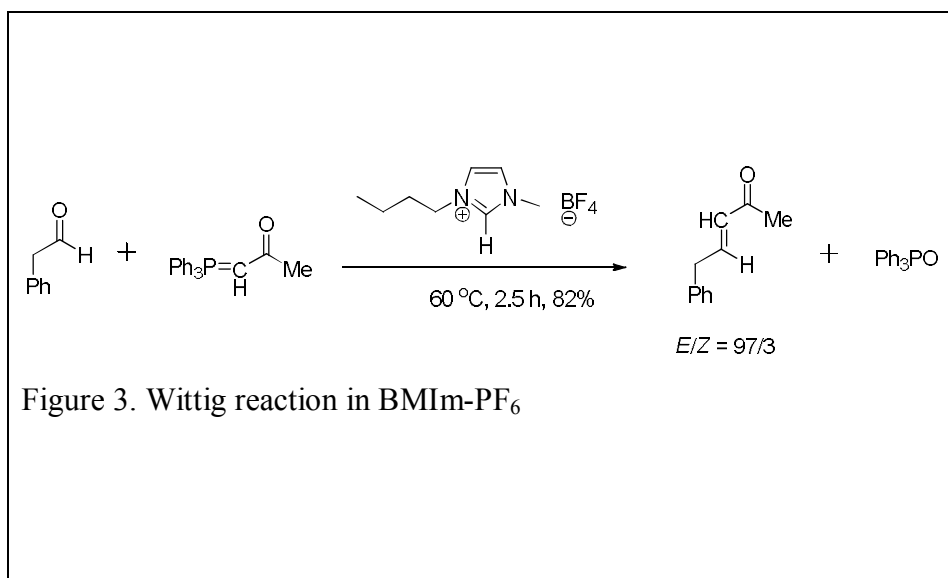
- (1) Negligible vapor pressure – Because ILs are composed of cation and anion, their vapor pressure are negligible, which related on the thermal stable leading to be used in harsh condition.
- (2) Designability – By a judicious combination of cations and anions, it is possible to adjust the solvent properties to the requirement of the reactions.
- (3) Polar non-coordinating solvent – Ionic species is polar but, poorly coordinating ion by combination of anions and cations. Thus, they have the potential to be high polar, yet non-coordinating, solvents.

(4) Reusability – ILs having appropriate composition are not miscible in organic solvent, which means that they are easy to separate and recycle.

Because of these properties of ILs, there are many applications into many fields, including organic and inorganic reaction, polymerization and industrial application.

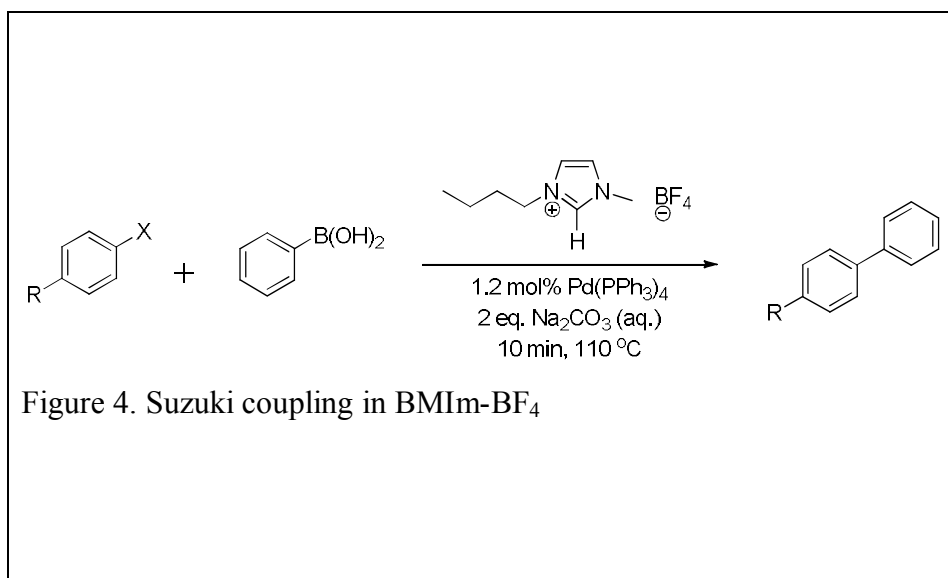
2.3.1.1 Wittig reaction

Wittig reaction is the mainly used in organic synthesis. It is having wider application as synthesis of the alkanes. The ionic solvent BMIm-BF₄ has been used as a medium to carry out Wittig reactions using stabilized ylides allowing easier separation of the alkenes from Ph₃PO and also recycling of the solvent. Further the E stereoselectivity was observed in the ionic liquid solvents, similar to that observed in organic solvents (Figure 3).⁶



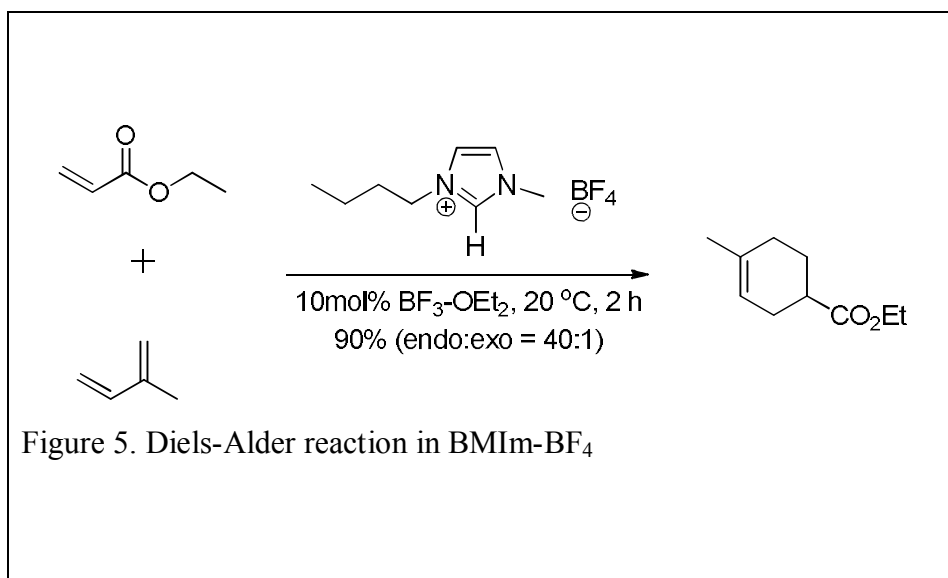
2.3.1.2 Suzuki coupling

The Suzuki coupling reaction (Figure 4) using Pd catalyst with ionic liquids found to be excellent yield and turnover numbers at room temperature. As compared to conventional Suzuki coupling reaction with ionic liquids proceed with high reaction rate. The reaction of bromo benzene with phenyl boronic acid under conventional Suzuki conditions gave 88% yield in 6 h, and with BMIm-BF₄ gave 93% yield in 10 min. The use of ultrasound in palladium with BMIm-BF₄ allowed the Suzuki coupling of various aryl halides with phenyl boronic acid to be conducted at room temperatures.⁶



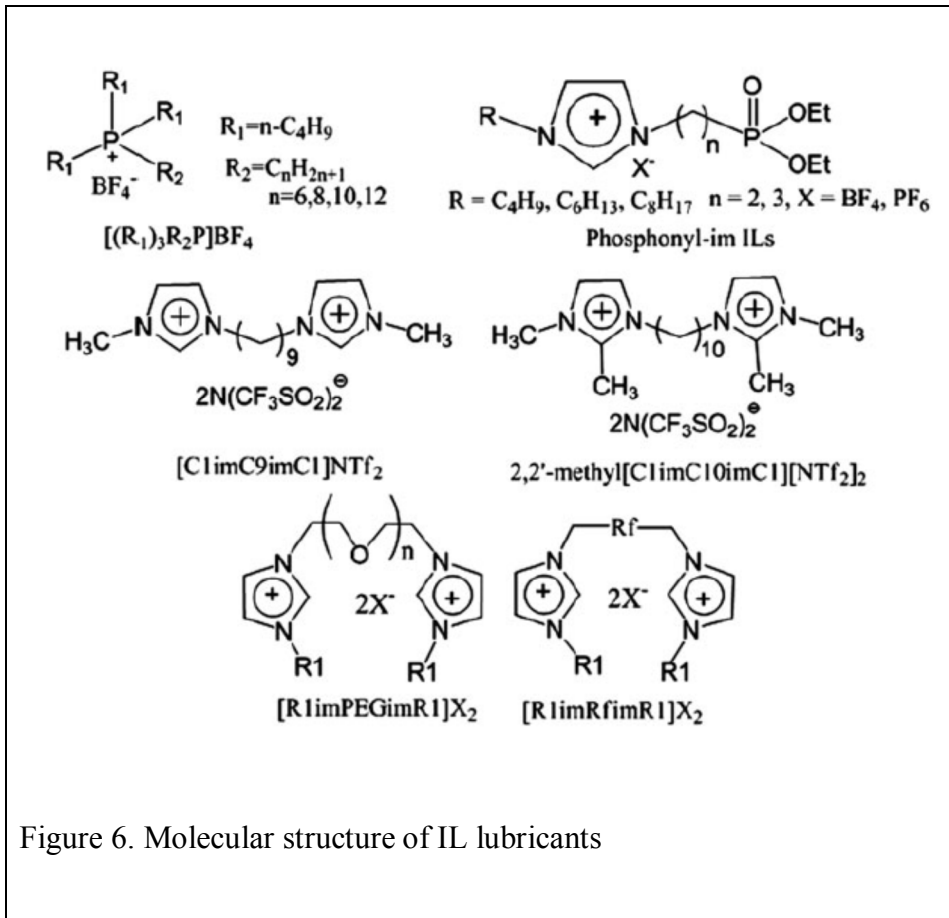
2.3.1.3 Diels–Alder reactions

It has found that Ionic liquids such as BMIm-BF₄ (Figure 5), BMIm-ClO₄, EMIm-CF₃SO₃, EMIm-NO₃, and EMIm-PF₆ were demonstrated as effective solvents for Diels–Alder reactions. The reaction between cyclopentadiene and methyl acrylate showed significant rate enhancements, high yields and strong endo selectivity's comparable with the best results obtained in conventional solvents.⁶



2.3.2 Lubricants

ILs possess a combination of unique characteristics, including negligible volatility, non-flammability, high thermal stability, low melting point, and conductivity. These properties have motivated research and led to various applications in many fields. On the other hand, these characteristics are also just what high performance lubricants demand. Very harsh friction conditions require lubricating oils to have high thermal stability and chemical inertness. The decomposition temperatures of imidazolium ILs are generally above 350 °C, some even as high as 480 °C, together with the low temperature fluidity means that ILs can function in a wide temperature range. The



most notable characteristic that distinguishes ILs from other synthetic lubrication oils is its high polarity.

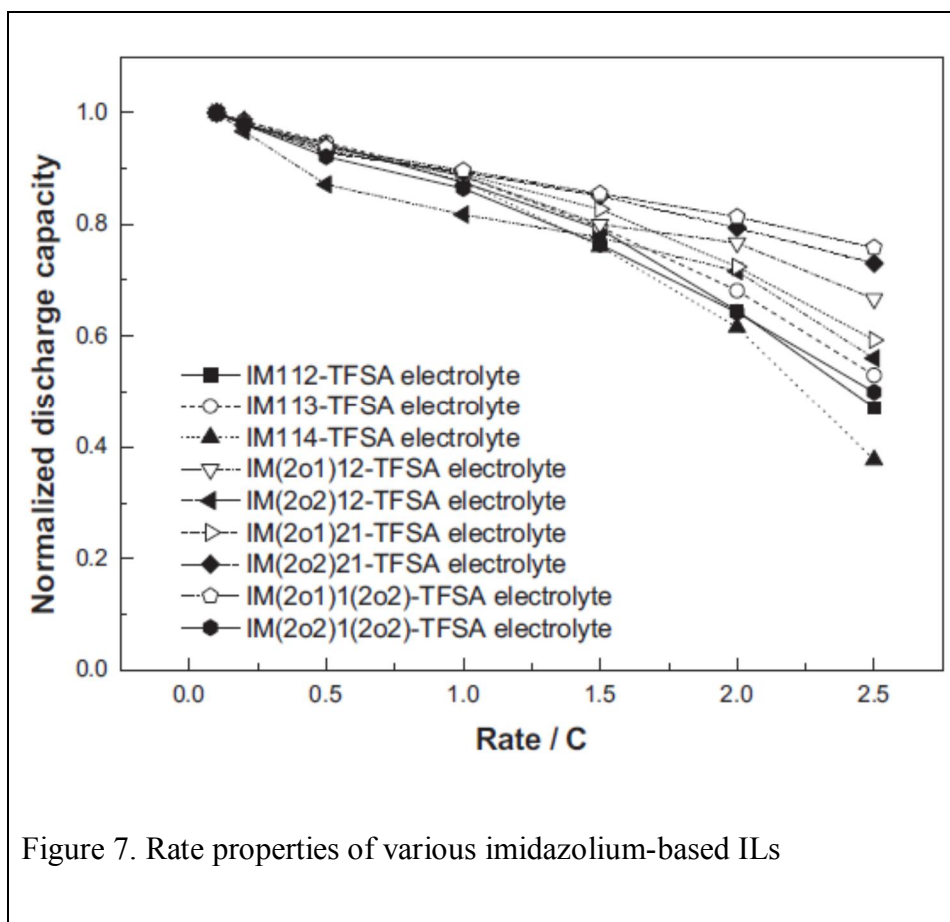
In this respect, the various ILs are used as lubricants and their application has expanded (Figure 6).⁷

2.3.3 Electrolytes for LIBs

Safety is a serious issue in lithium ion battery technology; consequently, many approaches are under study with the aim of reducing safety hazards. The electrolyte is the third component critical for the safety of lithium batteries. Concerns on the present LiFP_6 -organic carbonate solution electrolyte are:

- (1) the relatively narrow stability domain which prevents the use of high voltage cathodes
- (2) the high vapour pressure and the flammability which affects safety
- (3) the incompatibility with the environment and the human health, which results in serious manipulation hazards.

Due to these hazards, there are many attempts to replace the conventional carbonate as electrolytes for LIBs. In this trend, the ILs is an attractive material as electron media due to their unique properties. The ILs are salts that remain in liquid phase at room temperature even if they are composed of ionic species, cations and anions. Due to ionic interaction, they have unique properties such as high ionic conductivity, non-volatility, and non-flammability as well as a wide liquid range and wide electrochemical stability window.



Recently, interesting results were published by Hirano and co-workers.⁸ They reported the imidazolium cation structure by including ether moiety and removing the acidic proton of their C-2 position to obtain the useful ILs as electrolytes (Figure 7). In this case, the rate properties of imidazolium incorporated ether linkage had better performance. Due to the introducing the ether moiety in imidazolium ring, their electrochemically stability is increased than analogue of imidazolium-based ILs.

For the anion, the bis(fluorosulfonyl)imide (FSI) have been come into the spotlight in the field of electrolytes, due to their lower melting point and enhanced physical properties comparing to the bis(trifluoromethanesulfonyl)imide (TFSI). In this case, the FSI anion as a counter anion exhibits the lower viscosity and high ionic conductivity because the FSI anion is smaller than the TFSI anion in summarized Table 1.⁹

Table 1. Physical properties of FSI anion based ILs

	Neat RTILs	
	Viscosity (mPa s)	Conductivity (mS cm ⁻¹)
EMI[FSI]	18	15.4
Py ₁₃ [FSI]	40	8.2
PP ₁₃ [FSI]	95	3.7
EMI[TFSI]	33	8.3
Py ₁₃ [TFSI]	61	3.9
PP ₁₃ [TFSI]	151	1.4

In these results, it should be noted that application of ILs for LIBs is possible and ILs would be noticeable effect on both the safety issue and electrochemical performance.

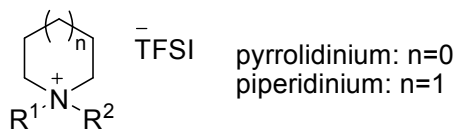
Results and Discussion

1. Synthesis and Properties of *N*-alkyl-2-methoxypyrrolinium bis(fluorosulfonyl)imide

1.1. Strategy

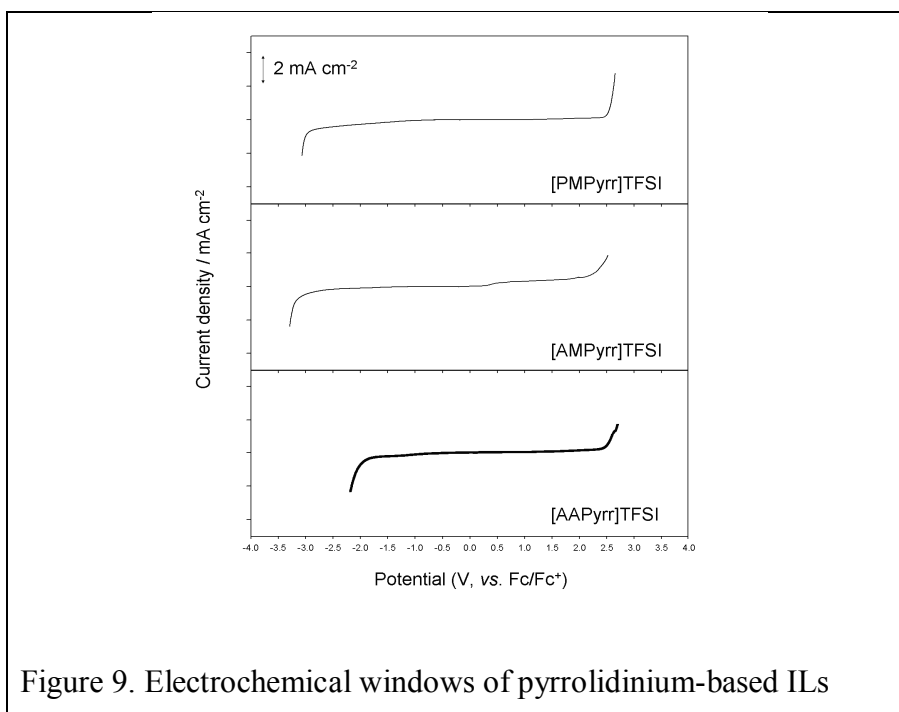
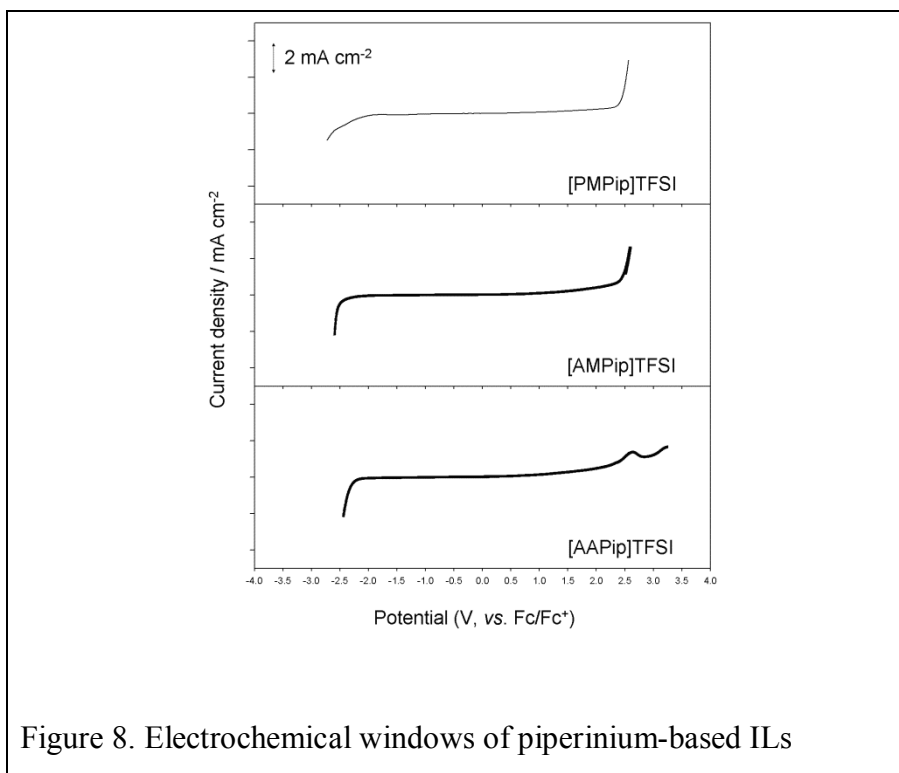
There have been many researches on controlling the physical and electrochemical properties of ILs via the alteration of their cation and anion. Among the previous study of ILs,⁵ the modification of imidazolium cations have been mostly focused due to its low melting points, lower viscosities, and higher ionic conductivities than other species derived from cyclic or acyclic amine. In our previous study, various ionic liquids from cyclic amine or acyclic amine such as imidazole, pyrrolidine, piperidine and acyclic amine have been investigated to improve their physical and electrochemical properties, which are designed by introducing functional groups. On the results from these studies, we realized that the structure of cations plays a significant role in physical and electrochemical properties. That is, introducing the alkyl substituent at C-2 position in the

Table 2. Physical properties of pyrrolidinium and piperidinium ionic liquids



Ionic liquids	η (cP)	σ (mS cm ⁻¹)
[PM]Pyrr-TFSI	59	4.9
[AM]Pyrr-TFSI	52	5.7
[AA]Pyrr-TFSI	57	4.6
[PM]Pip-TFSI	141	2.9
[AM]Pip-TFSI	108	3.5
[AA]Pip-TFSI	113	2.3

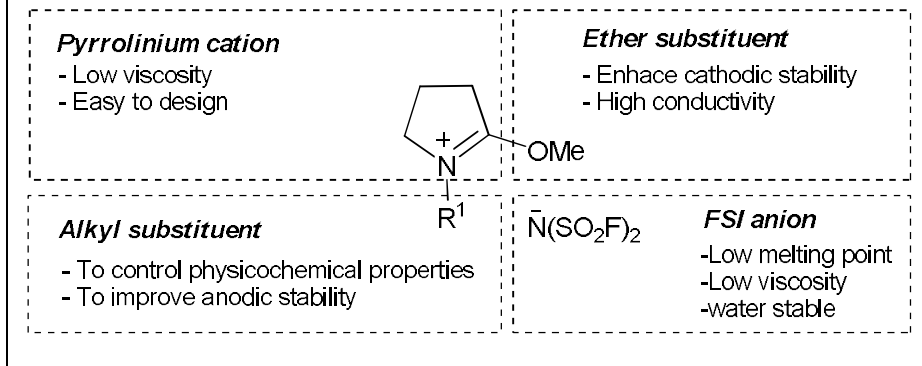
imidazolium-based ILs have a positive effect on the improvement of the cathodic stability, which means that the acidic proton at C-2 position of imidazolium ring structure derived its poor cathodic limit. Moreover, controlling the physical properties have been researched to change the ring size, that is, piperidinium-based ILs that have one more carbon than pyrrolidinium-based ILs showed higher viscosity and lower ionic conductivity compared to pyrrolidinium-based ILs, because larger cations increase Van Der Waals interactions and non-planarity of piperidinium-based ILs molecular structure does not allow a fairly facile slip between molecules.



Additionally, our group has investigated that the substituents of cation structure affect the physical properties to obtain the optimum structure of ILs. In this regards, we conclude that introducing the sp^2 carbon of double bond is effective to improve the ionic conductivity or electrochemical stability, due to more planar structure of double bond comparing to saturated carbohydrate. Moreover, the cation structure of ILs with the ether linkage is helpful to increase the ionic conductivity or lithium ion mobility because of the high binding affinity by a Lewis basic oxygen atom to a Lewis acidic Li^+ .

As an effort to develop novel electrolytes for electrochemical devices, we choose bis(fluorosulfonyl)imide (FSI) as a counter anion due to its lower melting point, lower viscosity, and higher stability in air and water.

Figure 10. Outline of the novel strategy; pyrrolinium-based ionic liquids with methoxy substituent.



To improve the physical and electrochemical performance, we suggested the pyrrolinium-based ILs with multi-functional groups as follows (Figure 10):

- (i) First, we expect that the planar sp^2 carbon of double bond would be beneficial to enhance physical properties of ILs because the planar structure as shown in imidazolium-based ILs allows rather facile slip between molecules, resulting in higher ionic conductivity as well as lower viscosity.
- (ii) Second, the additional C–O ether linkage would be advantageous for improving some physical properties together with Li^+ migration during electrochemical charging/discharging in that the relatively smaller C–O functional group reduces overall bulkiness of the IL, resulting in lower viscosity and higher ionic conductivity and the high binding affinity by a Lewis basic oxygen atom to a Lewis acidic Li^+ would enhance the Li^+ migration between electrodes, leading to better kinetic performance of the cell.
- (iii) Third, no acidic C–H proton as in the saturated pyrrolidinium-based ILs would be helpful to increase overall electrochemical stability of pyrrolinium-based ILs. It is well-known that the imidazolium-based ILs suffer from the continuous electrochemical decomposition as a result of the

irreversible reduction of the C–H proton at the C-2 position of an imidazolium ring.

- (iv) Lastly, bis(fluorosulfonyl)imide (FSI) anion were chosen owing to its lower melting point, lower viscosity, and higher stability in air and water.

1.2. Preparation

The pyrrolinium bis(fluorosulfonyl)imide with alkyl substituents was prepared according to the modified procedure described below (Scheme 1). The reaction was conducted with *N*-alkyl-2-pyrrolidinone and dimethyl sulfate to give corresponding *N*-alkyl-2-methoxypyrrolinium sulfate. Even if the *N*-propyl-2-pyrrolidinone and *N*-allyl-2-pyrrolidinone are commercial available, we synthesized these pyrrolidinone starting material due to their expensive cost.

The *N*-propyl and *N*-allyl-2-pyrrolidinone were synthesized by reaction between 2-pyrrolidinone and 1-bromopropane or allyl bromide in tetrahydrofuran (THF) solvent with sodium hydroxide at reflux condition for 24-48 h. The resulting crude *N*-alkyl-2-pyrrolidinone was evaporated under reduced pressure to remove THF and filtrate for removing the sodium hydroxide and purified by column

chromatography (dichloromethane : methanol= 10 : 1).

To obtain the pyrrolinium-based ILs, *O*-methylation of pyrroline ring was conducted with *N*-alkyl-2-pyrrolidinone and dimethyl sulfate in a neat condition. When the reaction was completed, the crude *N*-alkyl-2-methoxypyrrolinium monomethyl sulfate was washed with diethylether and ethyl acetate to remove organic impurities several times.

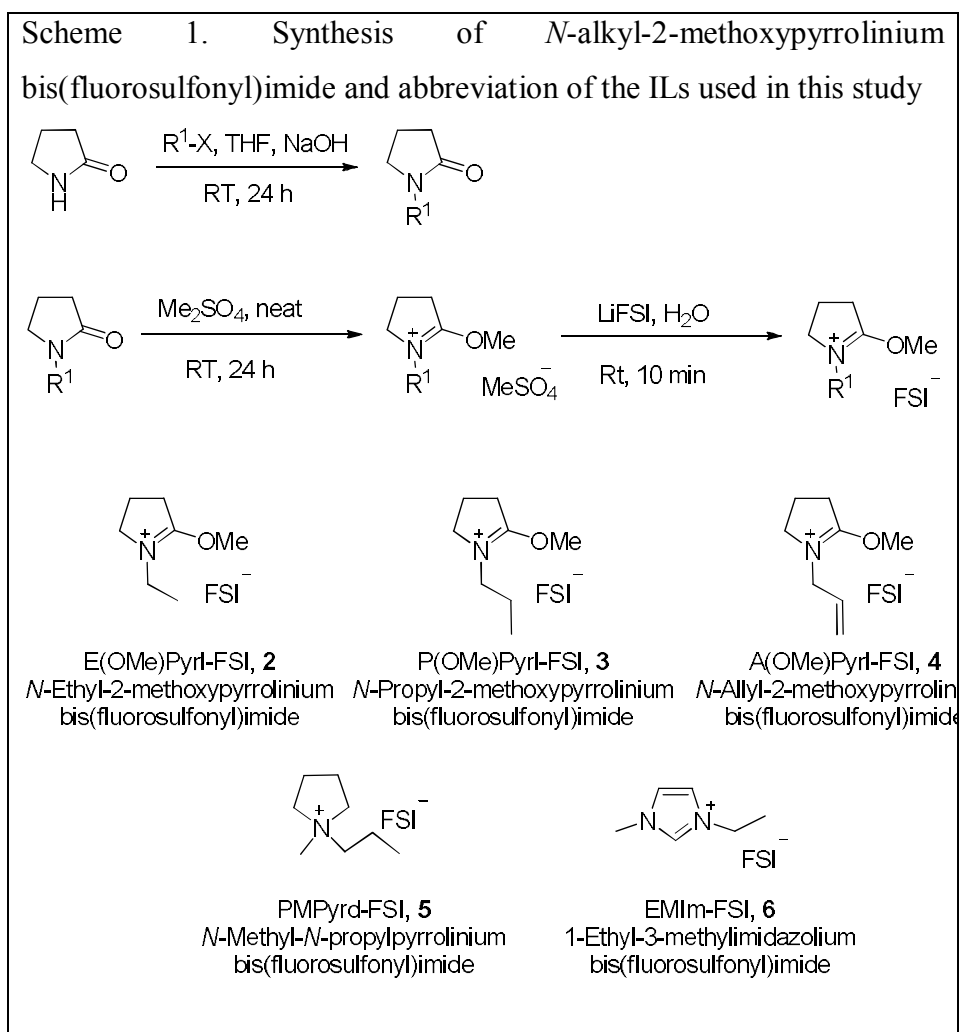
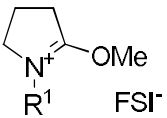


Table 3. Preparation of <i>N</i> -alkyl-2-methoxypyrrolinium bis(fluorosulfonyl)imide			
			
Entry	Compound	1st step(%)	2nd step(%)
1	M(OMe)PyrI-FSI	90	91
2	E(OMe)PyrI-FSI	91	93
3	P(OMe)PyrI-FSI	90	92
4	A(OMe)PyrI-FSI	89	91

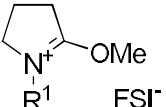
The crude *N*-alkyl-2-methoxypyrrolinium monomethyl sulfate was subjected to an anion exchange with lithium bis(fluorosulfonyl)imide (LiFSI) in water solution at room temperature for 10 mins. After this reaction was completed, distilled water was added and the product compound was extracted into dichloromethane. The separated organic layer was washed with fresh distilled water and dried MgSO₄, removed the organic solvent, and afforded the desired *N*-alkyl-2-methoxypyrrolinium bis(fluorosulfonyl)imide in 91-93 % yield (Table 3).

1.3. Thermal behaviors

Table 4 lists the thermal behavior such as T_c (crystallization point), T_m (melting point) and T_d (decomposition temperature) of the ILs prepared

in this research. Except the M(OMe)Pyr1-FSI, all of the pyrrolinium-based ILs exist the liquid phase at room temperature, and their melting point are below than 25 °C.

Generally, ILs is liquids phase at room temperature by controlling these three main factors,¹⁰ 1) the symmetries of cation and anion, 2) the interaction between cation and anion, and 3) the conformational flexibility of cation and anion, which implies that the structure of IL

Table 4. Thermal behaviors of pyrrolinium-based FSI ionic liquids					
					
No.	ILs	T_m (°C)	T_c (°C)	T_d (°C) ^a	Phase ^b
1	M(OMe)Pyr1-FSI	78	69	167	Solid
2	E(OMe)Pyr1-FSI	8	-15	159	Liquid
3	P(OMe)Pyr1-FSI	21	-31	165	Liquid
4	A(OMe)Pyr1-FSI	4	N.D ^c	150	Liquid

^a1 wt. % loss ^bphase at room temperature, ^cNot detected

could be designable to reduce the melting point and enhance the physical properties. Incorporating one ether group into the imidazolium, cyclic or acyclic quaternary ammonium and guanidinium cation has been proved to result the low melting points of the ILs,¹¹ because of reducing the symmetry of cations, lessening the interaction between the cation

and anion by electro-donating effect of ether group, and enhancing the flexibility of the cations. When bis(fluorosulfonyl)imide (FSI) is selected as anion of the prepared ionic liquids, the melting points of the ILs are reduced comparing to the bis(trifluorosulfonyl)imide (TFSI). The phase transition of these prepared ionic liquids were measured by differential scanning calorimetry (DSC), and it is noticeable that the *N*-ethyl-2-methoxypyrrolinium FSI (T_m : 9 °C) with high symmetry have lower melting point than *N*-methyl-2-methoxypyrrolinium FSI (T_m : 78 °C) or *N*-propyl-2-methoxypyrrolinium FSI (T_m : 21 °C) with lower symmetry.

Introducing an unsaturated substituent (C=C double bond of allyl) or sp^2 carbon of cation ring (pyrrolinium cation) would affect this observation that A(OMe)PyrI-FSI which is allyl-containing ILs decomposed at somewhat lower temperature than corresponding its analogue ILs such as P(OMe)PyrI-FSI. As in our previous work, the allyl-group-containing ILs showed less thermal stability than the corresponding ILs with propyl group. However, all of the pyrrolinium-based ILs were all thermally more stable than the conventional organic carbonate electrolyte such as dimethyl carbonate (DMC) (flash point: 18 °C, boiling point: 91°C) and ethylene carbonate (EC) (flash point: 160 °C, boiling point: 248 °C).

1.4. Physical properties

Tables 5 and 6 lists the viscosity (η) and ionic conductivity (σ) values of the pyrrolinium-based bis(fluorosulfonyl)imide with alkyl substituents. ,the viscosity value of analogue of imidazolium is even still lower (η = 19 cP at 25 °C and 11 cP at 50 °C for 1-ethyl-3-methylimidazolium FSI, η = 32 cP at 25 °C and 17 cP at 50 °C for *N*-ethyl-2-methoxypyrrolinium FSI), however, the analogue of pyrrolidinium is similar or higher than the pyrrolinium-based ILs (η = 40 cP at 25 °C and 19 cP at 50 °C for *N*-propyl-2-methoxypyrrolinium FSI, η = 40 cP at 25 °C and 21 cP at 50 °C for *N*-propyl-*N*-methylpyrrolidinium FSI). It is interesting that the viscosity of the *N*-allyl-2-methoxypyrrolinium FSI is lower than the analogue of propyl substituent due to the more planar structure of the A(OMe)Pyr1-FSI than the P(OMe)Pyr1-FSI (η = 30 cP at 25 °C and 14 cP at 50 °C for *N*-allyl-2-methoxypyrrolinium FSI, η = 40 cP at 25 °C and 19 cP at 50 °C for *N*-propyl-2-methoxypyrrolinium FSI).

Regarding the ionic conductivity, the lower viscosity of IL owned, the higher ionic conductivity of IL exhibited, consistent with the viscosity value, which means that the highest ionic conductivity was observed for the imidazolium-based ionic liquids. Although the P(OMe)Pyr1-FSI

have the lowest ionic conductivity ($\sigma = 8.4 \text{ mS cm}^{-1}$ without lithium salt at 25 °C) among the prepared ionic liquids, P(OMe)Pyr1-FSI ($\sigma = 4.8 \text{ mS cm}^{-1}$ with 1.0 M lithium salt at 25 °C) exhibit the similar value or higher value than PMPyrd-FSI ($\sigma = 4.7 \text{ mS cm}^{-1}$ with 1.0 M lithium salt at 25 °C) in practical condition of LIBs.

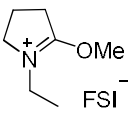
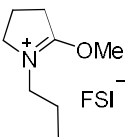
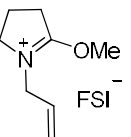
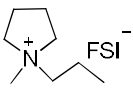
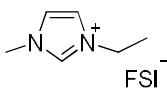
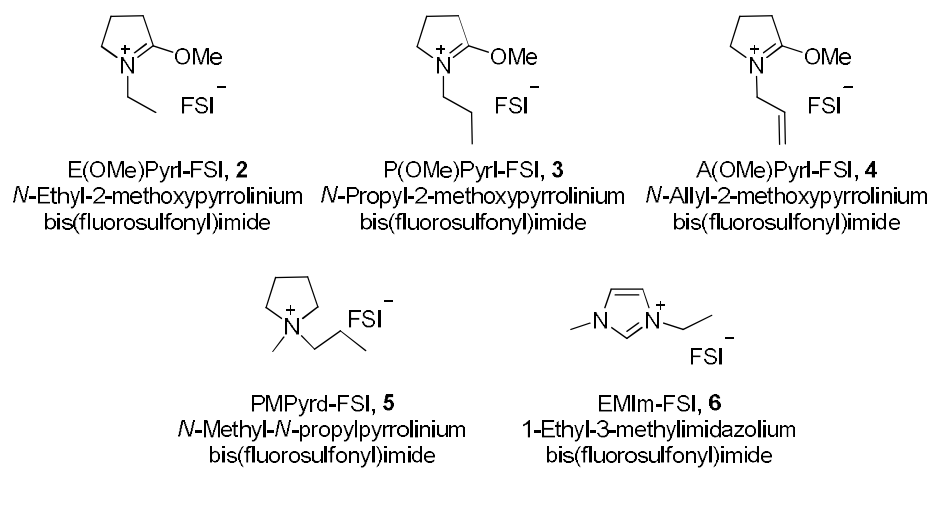
Table 5. Physical properties of pyrrolinium FSI ionic liquids					
<div style="display: flex; justify-content: space-around; align-items: flex-end;"> <div style="text-align: center;">  <p>E(OMe)Pyr1-FSI, 2 <i>N</i>-Ethyl-2-methoxypyrrolinium bis(fluorosulfonyl)imide</p> </div> <div style="text-align: center;">  <p>P(OMe)Pyr1-FSI, 3 <i>N</i>-Propyl-2-methoxypyrrolinium bis(fluorosulfonyl)imide</p> </div> <div style="text-align: center;">  <p>A(OMe)Pyr1-FSI, 4 <i>N</i>-Allyl-2-methoxypyrrolinium bis(fluorosulfonyl)imide</p> </div> </div>					
<div style="display: flex; justify-content: space-around; align-items: flex-end;"> <div style="text-align: center;">  <p>PMPyrd-FSI, 5 <i>N</i>-Methyl-<i>N</i>-propylpyrrolinium bis(fluorosulfonyl)imide</p> </div> <div style="text-align: center;">  <p>EMIm-FSI, 6 1-Ethyl-3-methylimidazolium bis(fluorosulfonyl)imide</p> </div> </div>					
No.	ILs	η (cP)		σ (mS cm ⁻¹)	
		25 °C	50 °C	25 °C	50 °C
2	E(OMe)Pyr1-FSI	32.1±0.2	17.1±0.2	13.1±0.1	16.7±0.1
3	P(OMe)Pyr1-FSI	40.0±0.3	19.1±0.2	8.3±0.1	13.4±0.1
4	A(OMe)Pyr1-FSI	30.1±0.1	14.0±0.1	10.3±0.1	16.3±0.1
5	PMPyrd-FSI	40.0±0.2	21.1±0.2	8.7±0.1	12.7±0.1
6	EMIm-FSI	19.1±0.2	11.0±0.1	15.7±0.1	19.1±0.2

Table 6. Physical properties of pyrrolinium FSI ionic liquids with 1.0 M lithium salt



No.	ILs	η (cP)		σ (mS cm ⁻¹)	
		25 °C	50 °C	25 °C	50 °C
2	E(OMe)Pyr1-FSI	52.1±0.2	22.1±0.1	5.3±0.2	11.3±0.2
3	P(OMe)Pyr1-FSI	56.1±0.3	25.9±0.2	4.8±0.2	8.3±0.2
4	A(OMe)Pyr1-FSI	42.1±0.2	21.2±0.2	5.2±0.1	10.9±0.2
5	PMPyrd-FSI	59.1±0.4	26.2±0.3	4.7±0.2	8.4±0.4
6	EMIm-FSI	30.1±0.3	16.1±0.2	10.3±0.2	15.7±0.2

1.5. Electrochemical Stability

The linear sweep voltammograms (LSV) of the pyrrolinium-based ILs with methoxy groups are shown in Figures 11 and 12. In cathodic limit of LSV performance in Figure 11, none of pyrrolinium-based

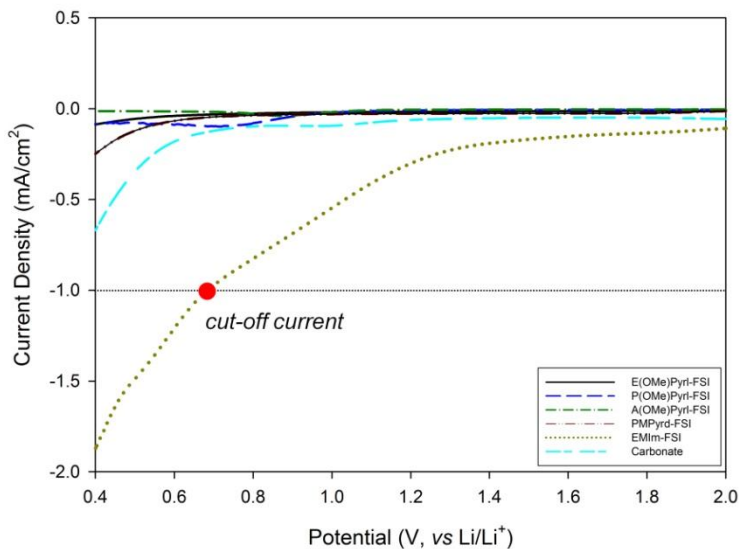


Figure 11. Cathodic limit of 6 different electrolytes; E(OMe)PyrI-FSI (black), P(OMe)PyrI-FSI (blue), A(OMe)PyrI-FSI (green), PMPyrd-FSI (red), EMIm-FSI (yellow), and carbonate (cyan)

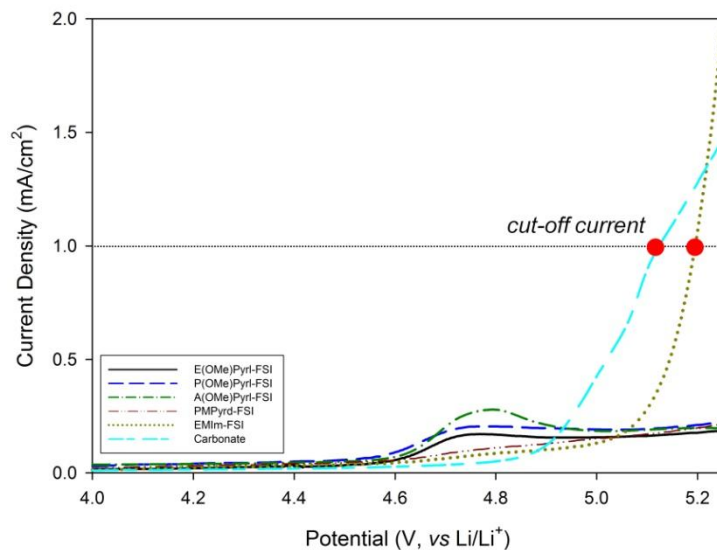


Figure 12. Anodic limit of 6 different electrolytes; E(OMe)PyrI-FSI (black), P(OMe)PyrI-FSI (blue), A(OMe)PyrI-FSI (green), PMPyrd-FSI (red), EMIm-FSI (yellow), and carbonate (cyan)

ionic liquids exhibit the significant current regardless of substituent, which implies that suggested pyrrolinium-cation have significantly positive effect on the cathodic polarization. It should be noted that all of the pyrrolinium-based IL are quite stable under the cathodic limit. Although the imidazolium-cation IL have the lowest viscosity and the highest ionic conductivity, a decrease of current density with the EMIm-FSI was showed at the 0.68 V (vs Li/Li⁺) with continuous decomposition of imidazolium. As already reported, several researches demonstrate that the acidic proton at the C-2 position in imidazolium ring affected electrochemical reduction in the cathodic limit, which result the poor electrochemical stability of the imidazolium cation.¹² The reduction peak of each electrolytes were observed at 0.7 V (vs Li/Li⁺), however, the peak of the commercially available carbonate exhibited unceasing decomposition whereas the peak of the pyrrolinium cation is restricted from additional decomposition.

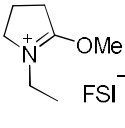
Comparing to the cathodic polarization, the anodic stability of the pyrrolinium-cation IL with the interesting behavior were observed with somewhat decomposition within effective current density (< 1mA cm⁻²). Generally, to enhance the electrochemical stability of the electrolytes, the double bond is incorporated in the modified cation. In the anodic limit, LSV behavior of the pyrrolinium-based IL exhibit stable performance without serious decomposition comparing to the EMIm-

FSI and commercially carbonate. As shown in Figure 12, the decomposition of commercially carbonate and EMIm-FSI were started at 5.12 V, and 5.20 V (vs Li/Li⁺), respectively, and their current density were gradually increased. However, there were different behaviors in the anodic stability of the modified pyrrolinium cation. When the alkyl substituent are introduced in the pyrrolinium-cation structure, the FSI anion decomposition is detected at 4.74 V (vs Li/Li⁺), however, the unceasing increase of oxidation peak is not observed in pyrrolinium-based ILs, which implies that the pyrrolinium-cation structure repress the gradually decomposition such as carbonate or EMIm-FSI.

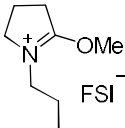
1.6. Electrochemical Performance

The charge-discharge processes of these prepared ILs with 1 C-rate were measured in the Li/LiFePO₄ half coin cell and the results are shown in Figures 13-15 and summarized in Table 7. As shown in Figures 13-15, all of the pyrrolinium-based IL exhibited the high discharge capacity and enhanced retention ratio comparing to the pyrrolidinium- and imidazolium-based ILs at 25 °C, respectively. The initial discharge capacity of the pyrrolinium-based IL is above 145 mAh g⁻¹, whereas that of the pyrrolidinium-based IL exhibits the low

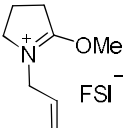
Table 7. Initial Discharge Capacity and Retention ratio of in six different electrolytes at 25 °C



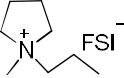
E(OMe)PyrI-FSI, 2
N-Ethyl-2-methoxypyrrolinium
bis(fluorosulfonyl)imide



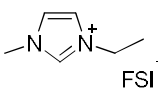
P(OMe)PyrI-FSI, 3
N-Propyl-2-methoxypyrrolinium
bis(fluorosulfonyl)imide



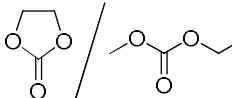
A(OMe)PyrI-FSI, 4
N-Allyl-2-methoxypyrrolinium
bis(fluorosulfonyl)imide



PMPYrd-FSI, 5
N-Methyl-*N*-propylpyrrolinium
bis(fluorosulfonyl)imide



EMIm-FSI, 6
1-Ethyl-3-methylimidazolium
bis(fluorosulfonyl)imide



Conventional Carbonate,
1.0 M LiPF₆ in EC/EMC
= 3/7 (V/V) + 3.0 wt% VC

No.	Electrolytes	Initial discharge capacity (mAh g ⁻¹)	Retention ratio at 50 th cycle (%)
2	E(OMe)PyrI-FSI	147.3	99.4
3	P(OMe)PyrI-FSI	144.8	98.6
4	A(OMe)PyrI-FSI	151.0	99.3
5	PMPYrd-FSI	127.5	99.8
6	EMIm-FSI	153.0	77.6
7	Carbonate	145.3	99.4

value (125 mAh g⁻¹). Moreover, It is interesting that retention ratio results of these three pyrrolinium-based ILs were more electrochemically stable than that of the EMIm-FSI (77.6% at 50th cycle in Table 7) although the imidazolium-cation have more positive effect on the physical properties than the pyrrolinium cation. Additionally, the rate performances of the coin cells with LFP cathode

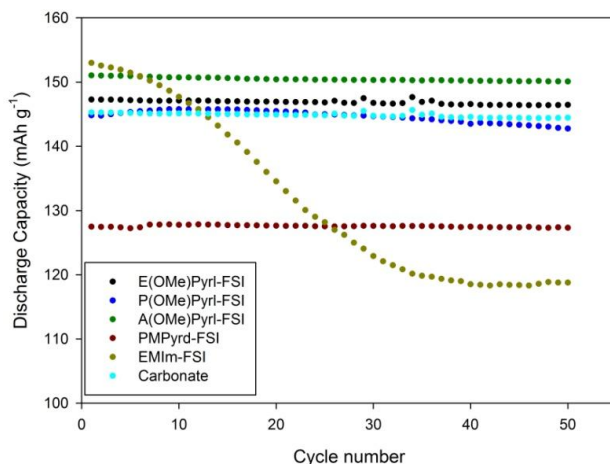


Figure 13. Cycle performance of the $\text{LiFePO}_4/\text{Li}^+$ cells in six different electrolytes at $25\text{ }^\circ\text{C}$; E(OMe)PyrI-FSI (black), P(OMe)PyrI-FSI (blue), A(OMe)PyrI-FSI (green), PMPyrd-FSI (red), EMIm-FSI (yellow), and carbonate (cyan)

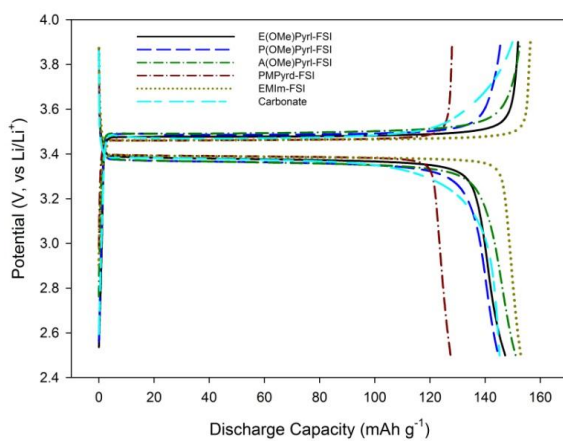


Figure 14. Potential profiles of the $\text{LiFePO}_4/\text{Li}^+$ cell in six different electrolytes at $25\text{ }^\circ\text{C}$ at the 1st cycle; (E(OMe)PyrI-FSI (black), P(OMe)PyrI-FSI (blue), A(OMe)PyrI-FSI (green), PMPyrd-FSI (red), EMIm-FSI (yellow), and carbonate (cyan)).

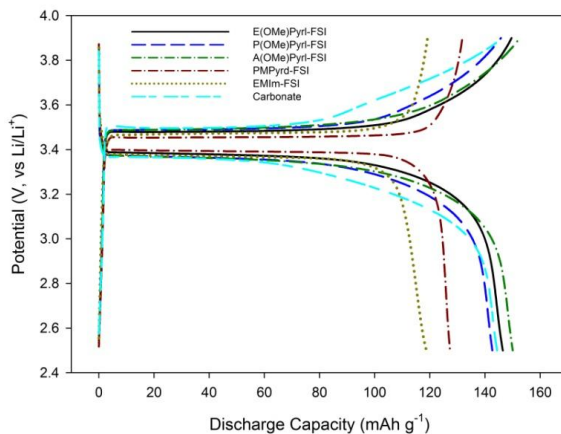


Figure 15. Potential profiles of the $\text{LiFePO}_4/\text{Li}^+$ cell in six different electrolytes at 25 °C at the 50th cycle; (E(OMe)PyrI-FSI (black), P(OMe)PyrI-FSI (blue), A(OMe)PyrI-FSI (green), PMPyrd-FSI (red), EMIm-FSI (yellow), and carbonate (cyan)).

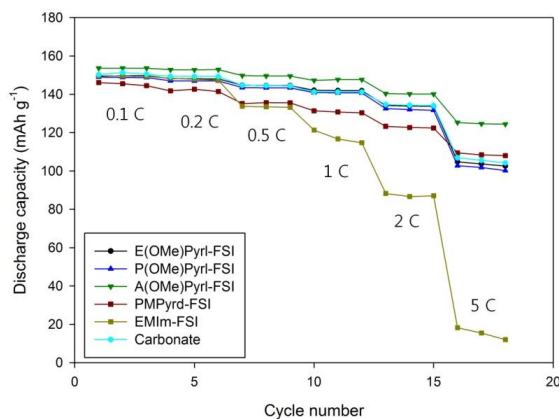


Figure 16. Rate performance of the $\text{LiFePO}_4/\text{Li}^+$ cell in six different electrolytes at 25 °C; (E(OMe)PyrI-FSI (black), P(OMe)PyrI-FSI (blue), A(OMe)PyrI-FSI (green), PMPyrd-FSI (red), EMIm-FSI (yellow), and carbonate (cyan)).

are shown in Figures 16-22 during the galvanostatic charge-discharge process from 0.1 C-rate to 5 C-rate. It is apparent that the discharge capacity of electrolytes decreased by increasing the C-rate. Especially, the rate performance of EMIm-FSI (Figure 21) exhibits the poor behavior, which could be affected by the reactive proton at C-2 position of imidazolium cation. The three electrolytes based on the pyrrolinium-cation with ether moiety (Figures 17-19) exhibit higher discharge capacity with the increasing current rate comparing to the other electrolytes, which implies that these results are attributed by the modified pyrrolinium structures with task-specific strategies of double bond (less viscosity), ether linkage (high ionic conductivity) and unstable acidic proton (enhanced electrochemical stability). Among the rate performances of the pyrrolinium cation ionic liquids, the allyl substituted cation shows the best result without serious decrease of discharge capacity as a result of the introducing an allyl substrate as more planar structure.

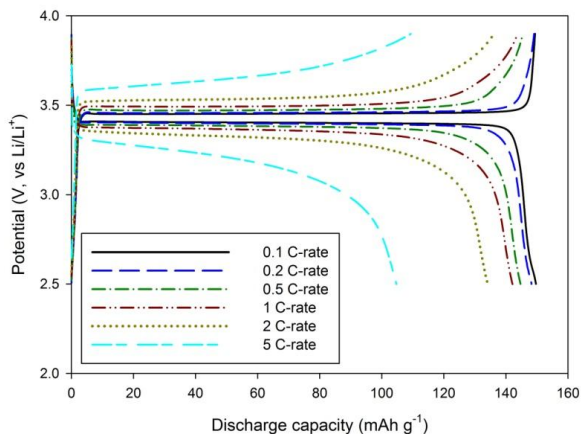


Figure 17. Potential profile of rate performance of the $\text{LiFePO}_4/\text{Li}^+$ cell in E(OMe)PyrI-FSI electrolytes at 25 °C from 0.1 C to 5 C (0.1 C-rate (black), 0.2 C-rate (blue), 0.5 C-rate (green), 1 C-rate (red), 2 C-rate (yellow), and 5 C-rate (cyan)).

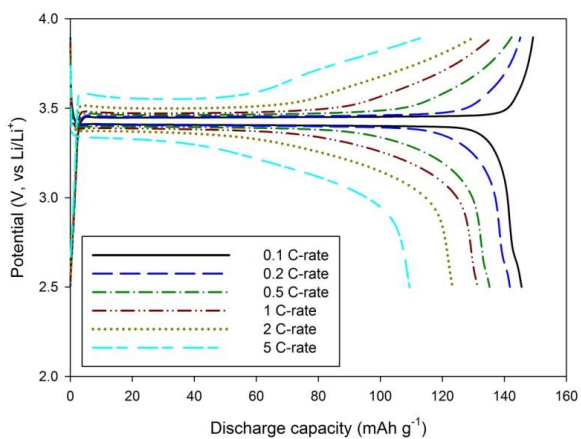


Figure 18. Potential profile of rate performance of the $\text{LiFePO}_4/\text{Li}^+$ cell in P(OMe)PyrI-FSI electrolytes at 25 °C from 0.1 C to 5 C (0.1 C-rate (black), 0.2 C-rate (blue), 0.5 C-rate (green), 1 C-rate (red), 2 C-rate (yellow), and 5 C-rate (cyan)).

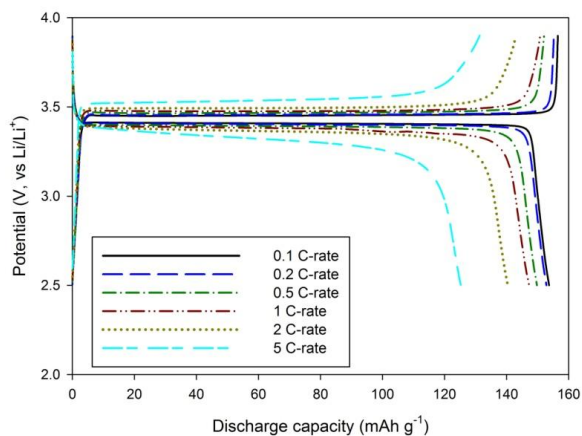


Figure 19. Potential profile of rate performance of the $\text{LiFePO}_4/\text{Li}^+$ cell in A(OMe)Pyr1-FSI electrolytes at 25 °C from 0.1 C to 5 C (0.1 C-rate (black), 0.2 C-rate (blue), 0.5 C-rate (green), 1 C-rate (red), 2 C-rate (yellow), and 5 C-rate (cyan)).

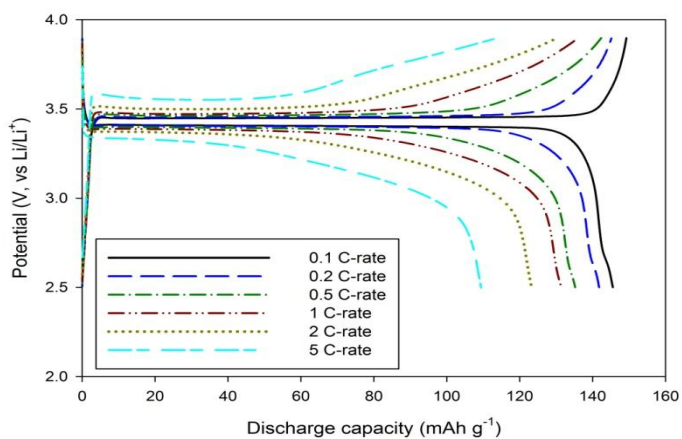


Figure 20. Potential profile of rate performance of the $\text{LiFePO}_4/\text{Li}^+$ cell in PMPyrd-FSI electrolytes at 25 °C from 0.1 C to 5 C (0.1 C-rate (black), 0.2 C-rate (blue), 0.5 C-rate (green), 1 C-rate (red), 2 C-rate (yellow), and 5 C-rate (cyan)).

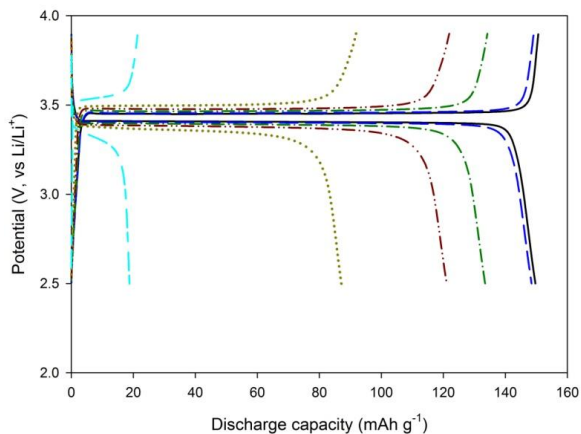


Figure 21. Potential profile of rate performance of the $\text{LiFePO}_4/\text{Li}^+$ cell in EMIm-FSI electrolytes at 25 °C from 0.1 C to 5 C (0.1 C-rate (black), 0.2 C-rate (blue), 0.5 C-rate (green), 1 C-rate (red), 2 C-rate (yellow), and 5 C-rate (cyan)).

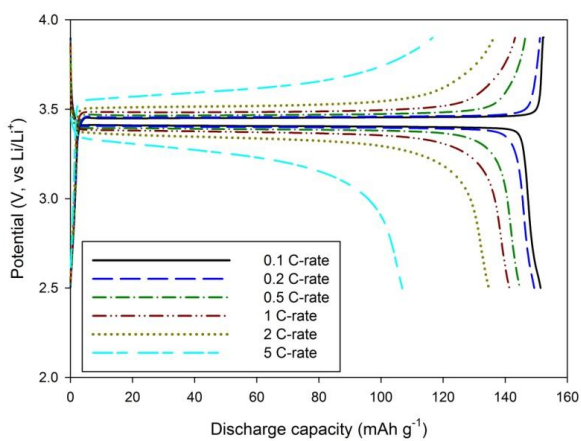

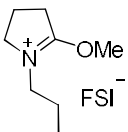
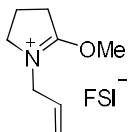
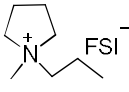
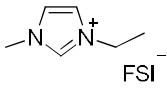
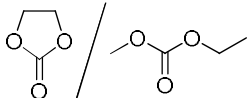


Figure 22. Potential profile of rate performance of the $\text{LiFePO}_4/\text{Li}^+$ cell in carbonate electrolytes at 25 °C from 0.1 C to 5 C (0.1 C-rate (black), 0.2 C-rate (blue), 0.5 C-rate (green), 1 C-rate (red), 2 C-rate (yellow), and 5 C-rate (cyan)).

Table 8. Lithium ion transference number of in six different electrolytes at 25 °C

		
E(OMe)PyrI-FSI, 2 <i>N</i> -Ethyl-2-methoxypyrrolinium bis(fluorosulfonyl)imide	P(OMe)PyrI-FSI, 3 <i>N</i> -Propyl-2-methoxypyrrolinium bis(fluorosulfonyl)imide	A(OMe)PyrI-FSI, 4 <i>N</i> -Allyl-2-methoxypyrrolinium bis(fluorosulfonyl)imide
		
PMPyrd-FSI, 5 <i>N</i> -Methyl- <i>N</i> -propylpyrrolinium bis(fluorosulfonyl)imide	EMIm-FSI, 6 1-Ethyl-3-methylimidazolium bis(fluorosulfonyl)imide	Conventional Carbonate, 7 1.0 M LiPF ₆ in EC/EMC = 3/7 (V/V) + 3.0 wt% VC
No.	Electrolytes	t_{Li^+}
2	E(OMe)PyrI-FSI	0.17
3	P(OMe)PyrI-FSI	0.14
4	A(OMe)PyrI-FSI	0.19
5	PMPyrd-FSI	0.14
6	EMIm-FSI	0.08
7	Carbonate	0.29

1.7. Summary

We have researched novel composition of the pyrrolinium cation and FSI anion to overcome the limitation of the conventional carbonate (thermal stability) and well-known ILs (disturbance of lithium ion mobility and electrochemical stability). The strategic cation from

organic and electrochemical aspects, pyrrolinium-based ionic liquids, was synthesized efficiently via 2 or 3 steps. As expected, these suggested ILs exhibited lower viscosity and higher ionic conductivity than pyrrolinium-based ILs as well as comparable electrochemical stability to the carbonate solution.

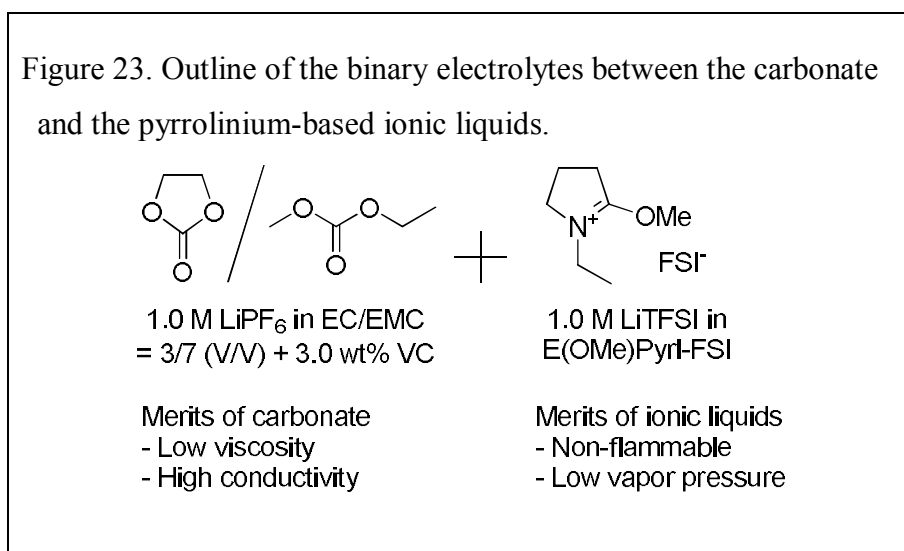
Among these pyrrolinium based ionic liquids are liquids at room temperature, except the M(OMe)PyrI-FSI, and the A(OMe)PyrI-FSI (**4**) exhibit lower value of viscosity (30.0 cP without lithium salt, 42.0 cP with lithium salt) and higher ionic conductivity value with lithium salt (5.2 mS cm^{-1}) than that of the analogue, P(OMe)PyrI-FSI, which would be reflected on introducing the planar structure as an allyl substrate. In regards of the LSV behaviors, all of the pyrrolinium-cation ILs was measured without serious decomposition comparing to the imidazolium-based IL, which would be implied by the effect of the reactive proton removal.

In terms of the electrochemical performance, the initial discharge capacity and retention ratio of these suggested ILs are close to that of the conventional carbonate solution, moreover, the electrochemical stability of the pyrrolinium-cation exhibit more stable than that of the pyrrolidinium and imidazolium-cation. Especially, the pyrrolinum ring with the unsaturated substituent (A(OMe)PyrI-FSI, **4**) shows the best result of rate performance without serious discharge decrease. It seems

to confirm that the pyrrolinium cation structure have a noticeable effect on both enhancing the physical properties and improving electrochemical stability.

2. Preparation and Properties of Binary Electrolytes

2.1. Strategy



Since the development of the pyrrolinium-based ILs, their properties have shown better electrochemical performance because of removing of the acidic proton and introducing the multi-functional groups. Nevertheless, the pyrrolinium-based ILs still suffer from high viscosity

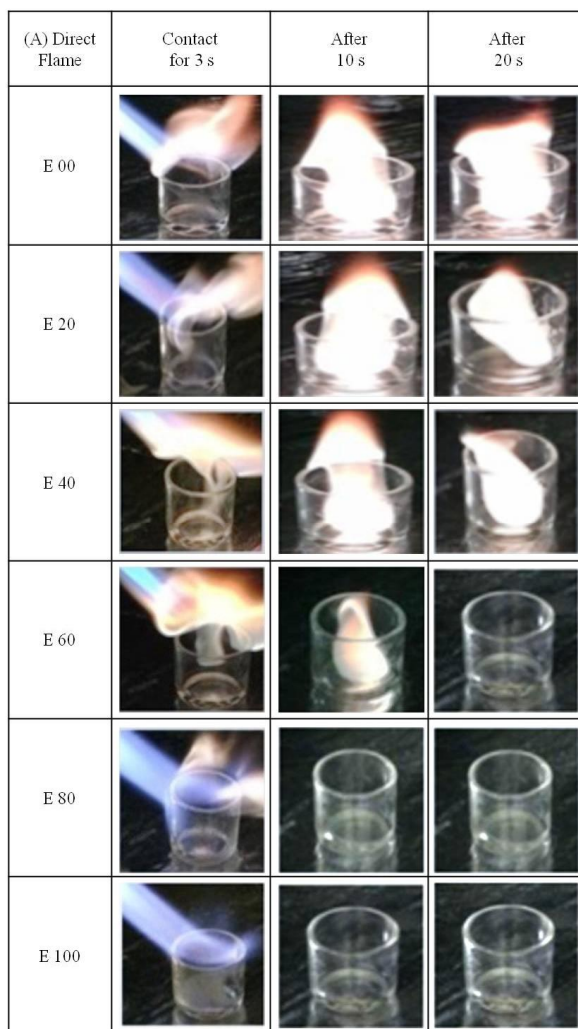
and low ionic conductivity, which would not be applied in LIBs. This limitation should be overcome to facilitate practical adoption of ILs as an electrolyte component for better electrochemical and safety performances of LIBs. As part of our ongoing study on utilizing pyrrolinium-based ILs as components for LIBs, we suggested the binary electrolyte systems that are composed of commercial carbonate-based electrolyte and the pyrrolinium-based IL to improve both the electrochemical and safety performance for LIBs (Figure 23). There have been recently reported a few binary electrolyte systems as an alternative approach to the conventional carbonated-based electrolytes and the noticeable enhancement of nonflammability of the mixed electrolytes was observed. However, those binary electrolyte systems would still have some critical limitations to be employed as an electrolyte for LIBs due to the base ILs used, which were imidazolium- or pyrrolidinium-based ILs. Those binary electrolytes suffer from poor cycling performance or inferior high rate performance, probably because of the poor electrochemical properties of the ILs employed. Herein, we have also compared the electrochemical properties of the pyrrolinium-based ILs with those of the imidazolium- or pyrrolidinium-based IL.

2.2. Preparation

Among the prepared pyrrolinium-based ILs, I choose the E(OMe)Pyr1-FSI due to their highest value of ionic conductivity (13.0 mS cm^{-1} at $25 \text{ }^\circ\text{C}$), which is related on the rate performance. Firstly, the 1.0 M lithium bis(trifluoromethanesulfonyl)imide (LiTFSI) is blended in the E(OMe)Pyr1-FSI to adjust balance of lithium concentration. Then, the mixtures were stirred for 10 min at room temperature and dried at $55 \text{ }^\circ\text{C}$ in vacuum oven for 8 hours for removing the water in ILs. It should be noted that we selected lithium bis(trifluoromethanesulfonyl)imide (LiTFSI) instead of lithium bis(fluorosulfonyl)imide (LiFSI) as a lithium salt for the electrolyte solution, because (1) LiTFSI has a similar chemical structure to LiFSI (compatibility with FSI-based ILs), (2) it is more resistive to the corrosion of a current collector,¹³ and (3) it is cheaper than LiFSI and commercially available. The mixture of E(OMe)Pyr1-FSI and commercially available carbonate (EC/EMC = 3/7 with 1.0 M LiPF_6 + 3.0 wt% VC) are mixed and investigated the viscosity, ionic conductivity, and electrochemical performance. The commercial carbonate as only electrolytes was measured to compare the physical and electrochemical properties of the ionic liquids.

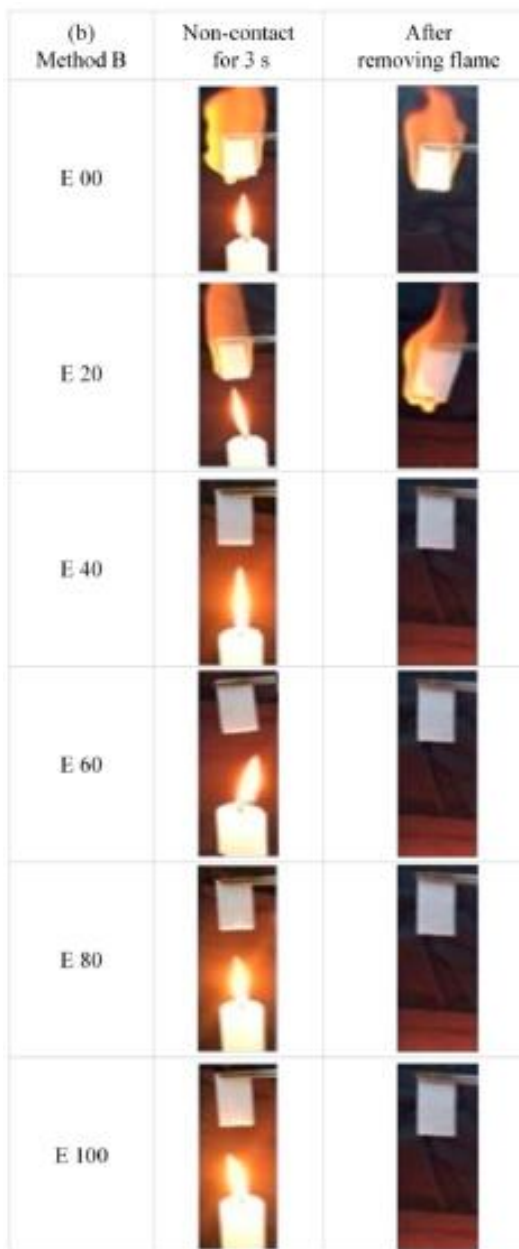
2.3. Flammability test

Figure 24. Images of the flammability tests of E 00, E 20, E 40, E 60, E 80, E 100 for direct flame combustion test (Method A)



To verify the flame-retarding effect of the pyrrolinium-based binary electrolytes, two kinds of flammability tests were performed as shown

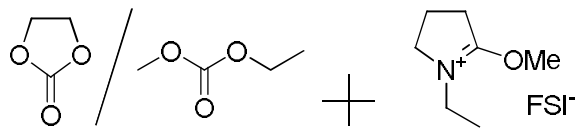
Figure 25. Images of the flammability tests of E 00, E 20, E 40, E 60, E 80, E 100 for indirect flame combustion test (Method B)



in Figures 24, 25 (see the Experimental Section for details). In a direct combustion test (Figure 24), the flammability of each binary electrolyte

depended mainly on the IL compositions and the binary electrolyte comprising 80 wt % or more of the IL did not ignite at all, whereas the binary electrolytes with or less than 60 wt % of the IL were combustible at the initial stage of ignition. However, the combustion feature seemed to be different after removal of the flame and the fire was gradually extinguished in the binary electrolytes with or more than 60 wt % of the IL. Similar results were observed in the other flammability test, which employed an indirect combustion method as shown in Figure 25. In contrast to the highly flammable behavior of the electrolyte with or less than 20 wt % of the IL, the higher contents of the IL made the binary electrolytes nonflammable probably because the pyrrolinium-based IL suppressed the flammable nature of the carbonate-based electrolytes. This is well consistent with the self-extinguishing time (SET) results in Table 9, which indicates the fire-extinguishing performance of each electrolyte. Addition of the pyrrolinium-based IL seemed effective to suppress the flammability of the carbonates-based electrolytes and the flammability was negligible in the binary electrolytes composed of 80 wt % or more of the IL and the SET values were greatly reduced with an increase of the IL contents. Note also that the time to extinguish a flame in the binary electrolyte with 60 wt % of the IL took only 5 s, whereas the binary electrolyte with 40 wt % of the IL showed the much longer SET value (30 s g⁻¹). It

suggests that the binary electrolyte with about 60 wt % of the pyrrolinium-based IL would be optimal when both the physical properties (viscosity and ionic conductivity) and the safety performance of the binary electrolyte are considered.

Table 9. Flammability Tests (Direct and Indirect Flame) and SET Values				
 <p>1.0 M LiPF₆ in EC/EMC = 3/7 (V/V) + 3.0 wt% VC 1.0 M LiTFSI in E(OMe)PyrI-FSI</p>				
No.	Electrolytes ^a	Method A (direct flame)	Method B (Indirect flame)	SET (s g ⁻¹)
1	E 00	O	O	103
2	E 20	O	O	45
3	E 40	O	X	30
4	E 60	O	X	5
5	E 80	X	X	
6	E 100	X	X	

^aE 00: a carbonate-only electrolyte, EC/EMC = 3/7 (V/V) with 1.0 M LiPF₆ and 3 wt % VC. E 100: an IL-only electrolyte, E(OMe)PyrI-FSI with 1.0 M LiTFSI. E 20, E 40, E 60, and E 80 are mixtures of E 00 and E 100 in different ratios, and contain 20, 40, 60, and 80 wt % of E 100 in each binary electrolyte, respectively.

2.4. Physical properties

The viscosity and ionic conductivity of the binary electrolytes are shown in Figures 26 and 27 and summarized in Table 10. The viscosity of the binary electrolytes seemed to be proportional to the composition of the IL and increased with an increase of the IL composition (Figure 27). As expected, a decrease in viscosity was observed at higher temperature (60 °C). The ionic conductivity of the binary systems seemed to be dependent on the IL composition (Figure 27). It showed the maximum value with 40 wt % of the IL (10.8 mS cm⁻¹ at 25 °C, 16.2 mS cm⁻¹ at 60 °C), and then gradually decreased as the IL content increased in the binary electrolyte systems. This trade-off effect seems to be attributed to the increased viscosity of the binary electrolytes with an increase of the IL. That is, the increase of the IL contents not only contributes to enhancement of overall ionic conductivity up to an optimal point but also results in an increase of viscosity of the electrolyte. Therefore, the mobility of ionic species seemed to be hindered once the IL content was over 40 wt %. This behavior could be explained by an inverse relationship between ionic conductivity and viscosity, i.e., the increase in the ionic conductivity by adding more ionic liquids results in the increase of the viscosity, which would decrease an overall mobility of the lithium ions in electrolyte

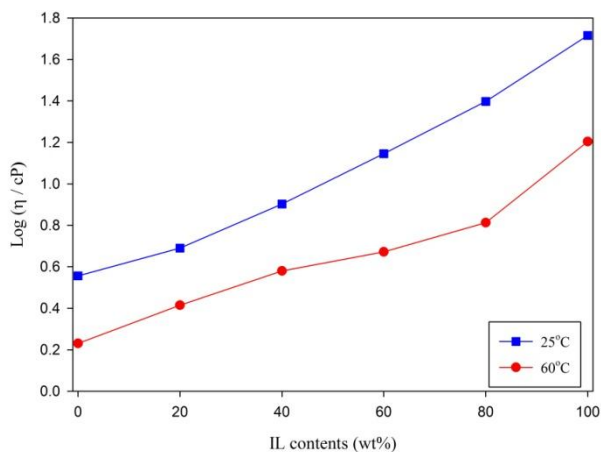


Figure 26. Viscosity of the binary electrolytes at 25 °C (blue) and 60 °C (red).

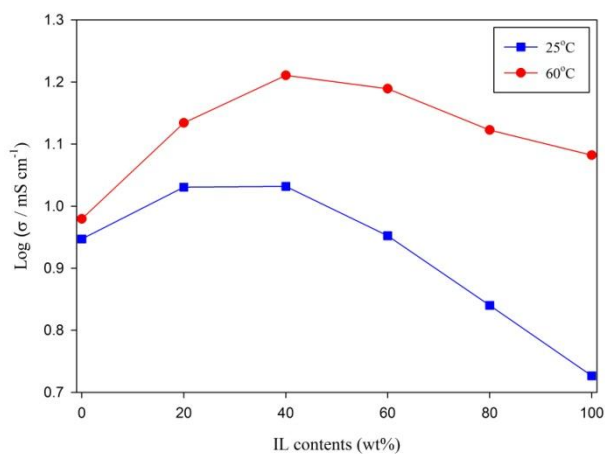
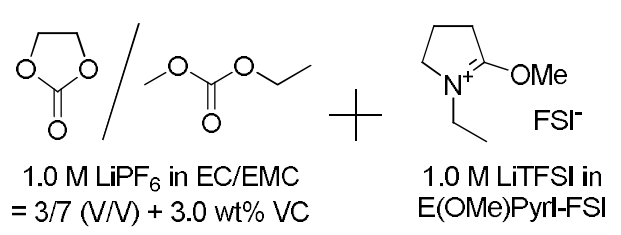


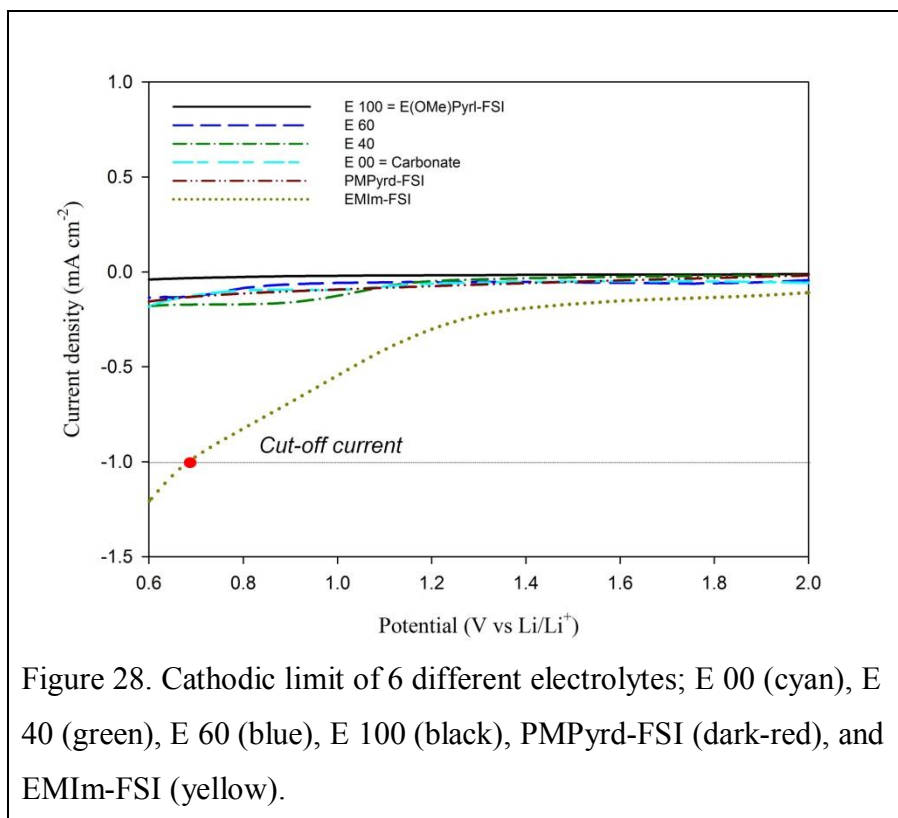
Figure 27. Ionic conductivity of the binary electrolytes at 25 °C (blue) and 60 °C (red).

after an optimal point.¹⁴ It is interesting to note that the pyrrolinium-based IL showed higher ionic conductivity (5.3 mS cm^{-1} with 1.0 M LiTFSI , 13.0 mS cm^{-1} without LiTFSI) than the pyrrolidinium-based IL (4.7 mS cm^{-1} with 1.0 M LiTFSI , 8.8 mS cm^{-1} without LiTFSI),⁹ but lower than the imidazolium-based IL (10.3 mS cm^{-1} with 1.0 M LiTFSI , 15.8 mS cm^{-1} without LiTFSI) at $25 \text{ }^\circ\text{C}$ (Table 10).⁹ The similar trend was also observed at $60 \text{ }^\circ\text{C}$.

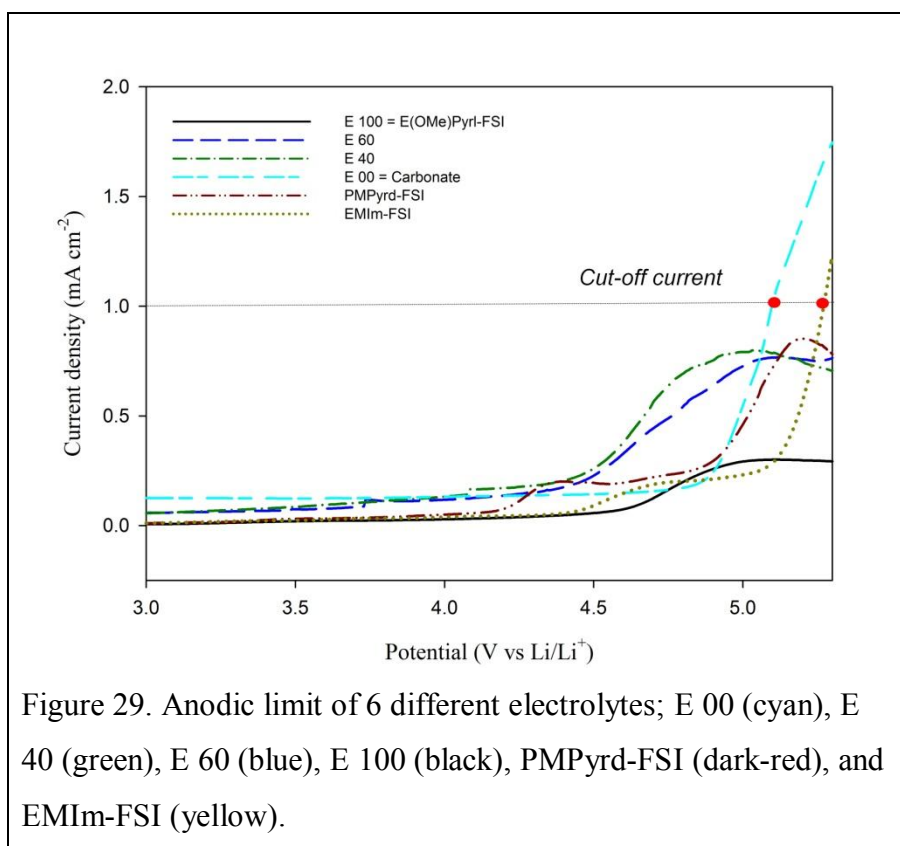
Table 10. Physical properties of binary electrolytes and ILs with 1.0 M lithium salt					
					
No.	Electrolytes	η (cP)		σ (mS cm^{-1})	
		$25 \text{ }^\circ\text{C}$	$60 \text{ }^\circ\text{C}$	$25 \text{ }^\circ\text{C}$	$60 \text{ }^\circ\text{C}$
1	E 00	3.6 ± 0.1	1.7 ± 0.1	8.8 ± 0.1	9.5 ± 0.2
2	E 20	4.9 ± 0.1	2.6 ± 0.1	10.7 ± 0.1	13.6 ± 0.1
3	E 40	8.2 ± 0.1	3.8 ± 0.1	10.9 ± 0.2	16.2 ± 0.2
4	E 60	14.2 ± 0.1	4.7 ± 0.1	9.0 ± 0.2	15.5 ± 0.2
5	E 80	25.0 ± 0.1	6.5 ± 0.1	6.9 ± 0.1	13.2 ± 0.2
6	E 100	52.1 ± 0.2	16.0 ± 0.2	5.3 ± 0.2	12.1 ± 0.1
7	PMPyrd-FSI	59.1 ± 0.4	23.1 ± 0.2	4.7 ± 0.2	9.5 ± 0.2
8	EMIm-FSI	30.1 ± 0.3	17.1 ± 0.3	10.3 ± 0.2	17.1 ± 0.1

2.5. Electrochemical Stability

To investigate electrochemical compatibility of the binary electrolytes systems, their electrochemical windows were examined by linear sweep voltammetry (LSV) as shown in Figures 28 and 29. In the LSV results for cathodic polarization, none of suggested binary electrolytes (from E 00 to E 100) showed significant currents within the effective current value ($\leq 1 \text{ mA cm}^{-2}$) regardless of the IL contents (Figure 28). This implies that all of the binary electrolytes have a similar cathodic stability in the typical potential range for cathodic



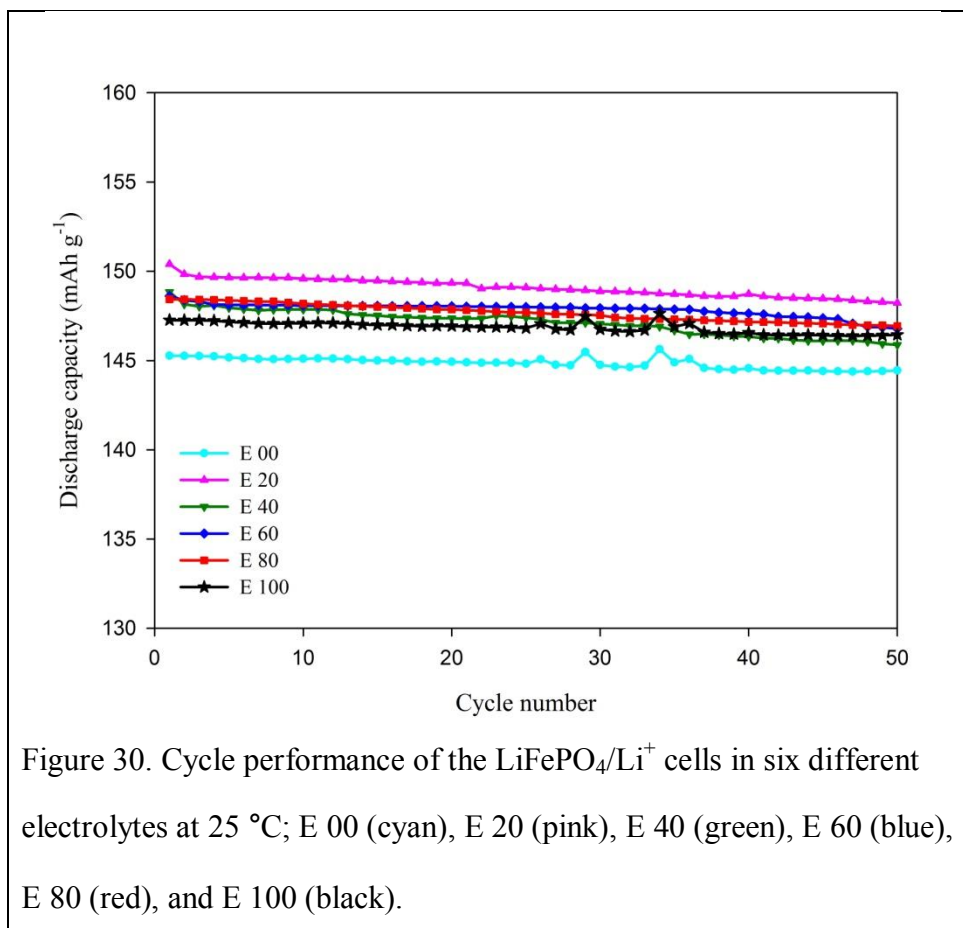
polarization. A noticeable point in the LSV results is that the cation structure of IL significantly affects overall cathodic stability. Note that all of the electrolytes composed of the pyrrolinium-based IL were quite stable under cathodic polarization. However, the imidazolium-based IL seriously suffered from continuous decomposition at 0.68 V (vs Li/Li⁺), which is highly associated with the cation structure of the IL. In practice, several previous studies demonstrated that existence of an acidic proton at the C-2 position of the imidazolium cation accelerated electrochemical reduction under cathodic polarization, resulting in poor



compatibility for conventional LIBs. These cathodic polarization results mean that the pyrrolinium cation is effective to improve the cathodic stability by removing the reactive C–H proton in the modified structure. In contrast to the cathodic stability, there was different electrochemical behavior in anodic stability with the binary electrolytes and the wider electrochemical stability was observed as increasing the IL contents (Figure 29). First, the anodic limits seemed to be more dependent on the IL contents and the electrochemical potential for initiation of electrolyte decomposition was gradually increased as the amount of the pyrrolinium-based IL in each binary electrolyte increased. For example, the decomposition of the carbonate-only electrolyte (E 00) started at around 5.1 V (vs Li/Li⁺), whereas some binary electrolytes with or more than 40 wt % of the pyrroliniumbased IL were stable over 5.2 V. In addition, further decomposition of the binary electrolytes (E 40 to E 100) seemed to be well-suppressed, whereas continuous electrolyte decomposition was observed with the carbonate-only electrolyte (E 00). Interestingly, they also showed an improved anodic stability compared to the known IL electrolytes such as the pyrrolidinium- and imidazolium-based ILs. According to the results of the anodic polarization, we presumed that the enhanced anodic stability could to be attributed the formation of a protective layer due to the unique structure of the pyrrolinium cation, which seems in line with the

previous results in literature.¹² Therefore, we suppose that the pyrrolinium-based IL allows the binary electrolytes to be more applicable to LIBs as they do not compromise their remarkable nonflammability with the electrochemical stability.

2.6. Electrochemical Performance



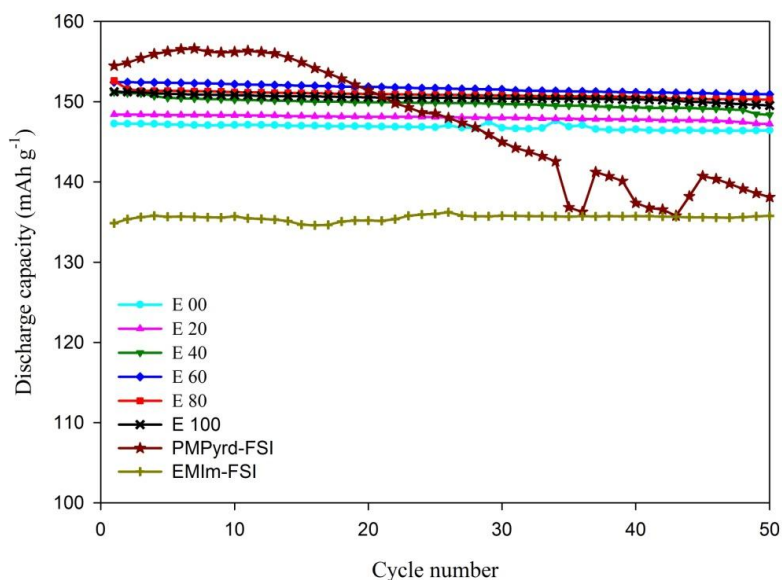


Figure 31. Cycle performance of the $\text{LiFePO}_4/\text{Li}^+$ cells in eight different electrolytes at $60\text{ }^\circ\text{C}$; E 00 (cyan), E 20 (pink), E 40 (green), E 60 (blue), E 80 (red), E 100 (black), PMPyrd-FSI (dark-red), and EMIm-FSI (yellow).

The electrochemical properties of the binary electrolytes were investigated and the results are shown in Figures 30-33 and summarized in Tables 11, 12. At $25\text{ }^\circ\text{C}$, all of the cells containing the binary electrolyte showed similar discharge specific capacity at around 150 mA h g^{-1} , which is almost identical to the specific capacity of LiFePO_4 (Figure 30). In addition, all of the binary electrolytes with the pyrrolinium-based IL showed stable galvanostatic charge–discharge processes that the cells cycled with the binary electrolytes still had high specific capacities over 145 mA h g^{-1} (more than 98.0% of specific

capacity retention) at the end of cycling at both 25 and 60 °C, regardless of the pyrrolinium-based IL contents (Figures 30 and 31). Note also that the pyrrolinium-based binary electrolytes exhibited an improved electrochemical performance compared to the imidazolium- and pyrrolidinium-based ILs (Figure 31). The cell cycled with the pyrrolinium-based IL only electrolyte showed a higher initial specific capacity than the pyrrolidinium containing cell (151.3 mA h g⁻¹ (E 100) vs 134.9 mA h g⁻¹ (PMPyrd-FSI) at the 50th cycle at 60 °C, see the

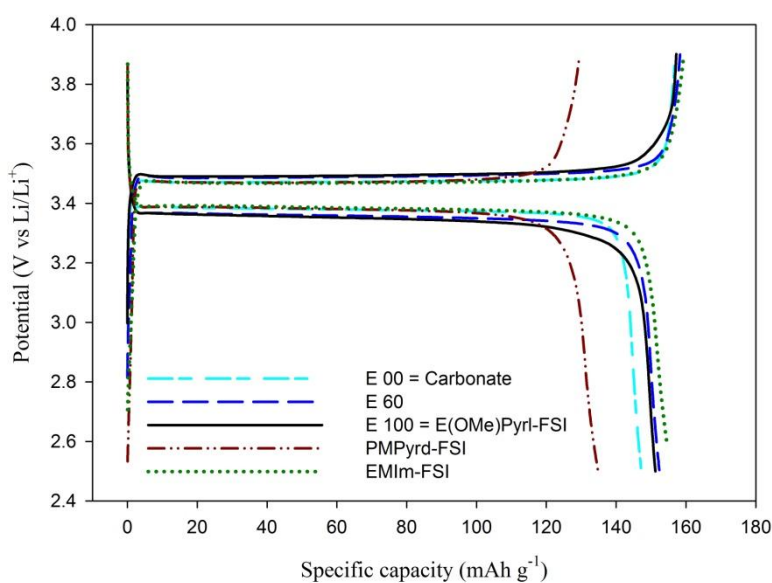


Figure 32. Potential profiles of the LiFePO₄/Li⁺ cell in five different electrolytes at 60 °C at 1st cycle; E 00 (cyan), E 60 (blue), E 100 (black), PMPyrd-FSI (dark-red), and EMIm-FSI (yellow).

Table 12) and exhibited a better cycling performance than the imidazolium-containing cell (98.9% (E 100) vs 89.4% (EMIm-FSI) at the 50th cycle at 60 °C, see the Table 12). It could be attributed to the task-specific structure of the pyrrolinium cation characterized by the sp^2 carbon of double bond (lower viscosity), the C–O ether linkage (higher ionic conductivity), and excluding an unstable C–H bond (wider electrochemical window). In practice, the lithium ion transference number (t_{Li^+}) of electrolytes, which is responsible for the migrating rate of Li^+ ions, was mainly dependent on the cation structure

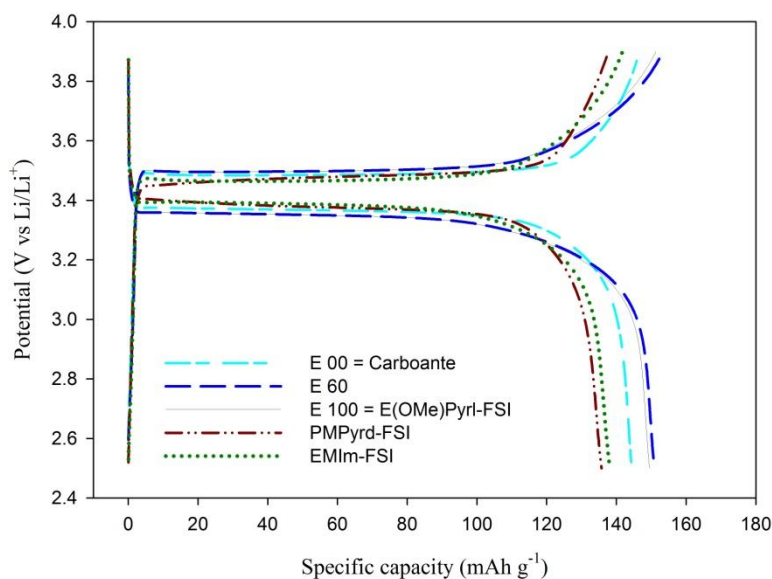


Figure 33. Potential profiles of the $LiFePO_4/Li^+$ cell in five different electrolytes at 60 °C at 50th cycle; E 00 (cyan), E 60 (blue), E 100 (black), PMPyrd-FSI (dark-red), and EMIm-FSI (yellow).

of the ILs and the multifunctionalized E(OMe)PyrI-FSI showed higher t_{Li^+} than either PMPyrd-FSI¹⁵ or EMIm-FSI (Table 8). It implies that the pyrrolinium cation plays an important role to enhance the overall electrochemical performance of the cell as well as the safety issues in LIBs.

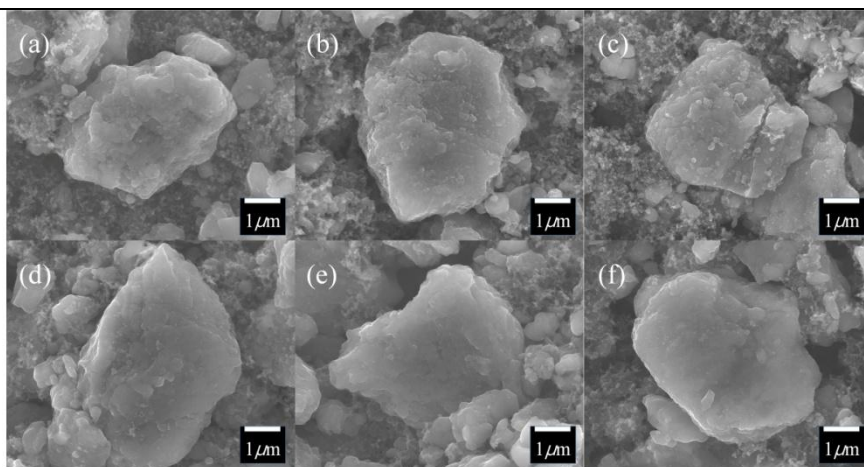
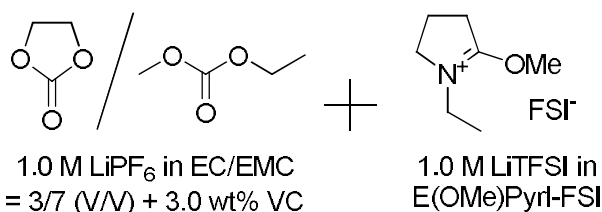


Figure 34. SEM images of the LiFePO_4 cathode in each binary electrolyte after the 50th cycle between 2.5 and 3.9 V (vs Li/Li^+) at 60 °C; (a) E 00, (b) E 20, (c) E 40, (d) E 60, (e) E 80, and (f) E 100.

Further SEM analysis provided an informative clue to estimate effectiveness of the binary electrolytes. The surface morphologies of the LiFePO_4 electrodes cycled between 2.5 and 3.9 V (vs Li/Li^+) were almost similar to each other without any evidence of the electrolyte decomposition (Figure 34). It seems to confirm that the proposed

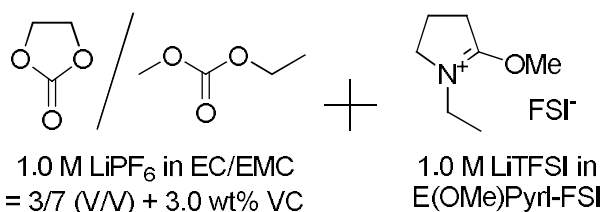
Table 11. Initial Discharge Capacity and Retention ratio of in six different electrolytes at 25 °C



No.	Electrolytes	Initial discharge capacity (mAh g ⁻¹)	Retention ratio at 50 th cycle (%)
1	E 00	145.3	99.4
2	E 20	150.4	98.5
3	E 40	148.8	98.0
4	E 60	148.6	98.8
5	E 80	148.4	99.0
6	E 100	147.3	99.4

approach with the binary electrolytes based on the combination of the pyrrolinium-based IL with the carbonate solvent would be effective to achieve an excellent safety performance of the cell together with a good cycling performance without any trade-off effect.

Table 12. Initial Discharge Capacity and Retention ratio of in eight different electrolytes at 60 °C



No.	Electrolytes	Initial discharge capacity (mAh g ⁻¹)	Retention ratio at 50 th cycle (%)
1	E 00	147.3	99.4
2	E 20	148.4	99.2
3	E 40	151.2	98.1
4	E 60	152.4	99.0
5	E 80	152.6	98.5
6	E 100	151.3	98.9
7	PMPyrd-FSI	134.9	99.9
8	EMIm-FSI	154.5	89.4

2.7. Summary

We have developed new binary electrolytes that consist of the pyrrolinium-based IL and commercial carbonate to address the safety issues in LIBs as well as to overcome the disturbance of lithium ion mobility. The task-specific compound, pyrroliniumbased IL (E(OMe)Pyr1-FSI), was synthesized efficiently and the corresponding

binary electrolyte systems were prepared by changing the ratios between the pyrrolinium-based IL and commercial carbonate. The newly prepared binary electrolytes showed significant fire-retarding results and enhanced physical properties as well as comparable electrochemical performance to the commercial carbonate electrolyte.

Among the prepared binary electrolyte systems, those with 40 and 60 wt % of the IL are considered as an optimal range because they have much improved fire-retarding characteristics as well as large ionic conductivity values (16.2 mS cm^{-1} for E 40, 15.5 mS cm^{-1} for E 60 at $60 \text{ }^\circ\text{C}$). Especially, the inflammable nature of the IL has a drastic decreasing effect on the SET values for the binary electrolytes with 60 wt % or more of the IL.

In terms of the electrochemical stability, the initial discharge capacity and retention ratio of the pyrrolinium-based binary electrolytes are nearly identical with that of the commercial carbonate as an only electrolyte solvent. Furthermore, the electrochemical performance of the pyrrolinium-IL only electrolyte at 1 C rate exhibits the outstanding stability with the LiFePO_4 cathode than that of the pyrrolidinium- or imidazolium-IL only electrolyte. Moreover, the SEM analysis of the morphologies of the active material (LiFePO_4) in each binary electrolyte (the 50th cycle at $60 \text{ }^\circ\text{C}$) provided another proof that the binary electrolytes were stable during the galvanostatic

charge–discharge process under harsh conditions. It seems to confirm that the binary electrolytes prepared from the pyrrolinium-based IL and carbonate solvent have a noticeable synergistic effect on both the fire-retarding characteristics and electrochemical properties.

Conclusion

In the work for development of pyrrolinium-based ILs as an alternative electrolyte for lithium ion batteries (LIBs), we modified the substituent on the pyrrolinium cation ring and introduced the multi-functional group with sp^2 carbon, ether linkage, and removal of acidic proton to enhance the physical and electrochemical performances. Additionally, the bis(fluorosulfonyl)imide (FSI) anion is used as a counter anion to their low melting point and chemical stability.

The pyrrolinium FSI ILs with 2-methoxy group were synthesized and their thermal behaviors and physical properties are measured. Except the M(OMe)Pyr1-FSI (**1**), all of the pyrrolinium FSI ILs are liquid phase at room temperature. The prepared IL with an allyl substituent were thermally less stable than its analogue ILs with a propyl substituent, however they were still more stable than conventional carbonate such as ethylmethyl carbonate (EMC) or ethylene carbonate (EC). The physical properties of pyrrolinium-based ILs are similar or better than propylmethylpyrrolidinium bis(fluorosulfonyl)imide (PMPyrd-FSI, **5**), especially, the *N*-ethyl-2-methoxypyrrolinium bis(fluorosulfonyl)imide (E(OMe)Pyr1-FSI, **2**) exhibit the best value of ionic conductivity (13.0 mS cm^{-1}) among the pyrrolinium-based ILs. To investigate the electrochemical stability of synthesized ILs in this work,

we measured the linear sweep voltammogram (LSV). All of the pyrrolinium-based ILs are electrochemically stable than 1-ethyl-3-methylimidazolium bis(fluorosulfonyl)imide (EMIm-FSI, **6**) due to the no active proton in cation ring. In the electrochemical performance, all of the pyrrolinium-based ILs are similar results comparing to the conventional carbonate, which implies that these ILs are compatibility to the electrolyte for LIBs. Whereas the PMPyrd-FSI (**5**) and EMIm-FSI (**6**) exhibit the low capacity and fading effect on the LiFePO₄ electrode, which means that there are helpful to apply the practical LIBs through structure modifications with task-specific functionalities such as the sp² carbon of double bond, the C-O ether linkage, and no unstable proton.

To allow the pyrrolinium-based ILs to be more applicable the LIBs, we suggested the binary electrolytes systems between the E(OMe)Pyr1-FSI (**2**) and conventional carbonate (1.0 M LiPF₆ in EC/EMC=3/7 with 2.0 wt% VC). To verify the flame-retarding effect of the E(OMe)Pyr1-FSI (**2**), two kinds of flammability tests were perfumed and their results are that the flammability of each binary electrolytes are depended on the composition of the IL. In a direct combustible test, the binary electrolytes comprising 80 wt% or more of the IL did not ignite at all, however, self extinguish time (SET) of electrolyte with the 60 wt% IL content are drastically reduced to 5 s g⁻¹. Also, the physical properties

of these electrolytes systems are optimum range 40 wt% to 60 wt% of the IL because they have improved fire-retarding characteristics as well as large conductivity values (16.2 mS cm^{-1} for E 40, 15.5 mS cm^{-1} for E 60 at $60 \text{ }^\circ\text{C}$). In terms of the electrochemical performance, the initial discharge capacity and retention ratio of the pyrrolinium-based binary electrolytes are closely to that of the conventional carbonate (E 100).

To sum up, the pyrrolinium-based ILs enhanced the physical and electrochemical properties due to their task-specific modification such as sp^2 carbon, ether moiety and no acidic proton. Comparing to well-known ILs, the results of properties imply that the cation structure of IL has a significant effect on their performances, which means that the pyrrolinium-based ILs are more applicable to be used as electrolytes for LIBs. On the extension of these results, the binary electrolytes composed of pyrrolinium-based ILs and conventional carbonate have an impressive synergetic effect on both the fire-retarding property and electrochemical stability owing to the cation structure of pyrrolinium-based IL.

Experimental Details

1. General

Materials were purchased from commercial suppliers and used without further purification. *N*-Ethyl-2-pyrrolidone, 2-pyrrolidinone, 1-bromopropane, allyl bromide and dimethyl sulfate were distilled under reduced pressure immediately prior to use. Even if the *N*-propyl-2-pyrrolidinone and *N*-allyl-2-pyrrolidinone are commercial available, we synthesized these pyrrolidinone starting materials. All experimental glassware, syringes, and magnetic stirring bars were oven-dried and stored in a desiccator before use. PMPyrd-FSI and EMIm-FSI (Scheme 1) were synthesized as described in a previous report.⁹

¹H and ¹³C NMR spectra were obtained in CDCl₃ on a Bruker Avance III spectrometer (400 MHz for ¹H and 100 MHz for ¹³C NMR). The ¹H NMR spectroscopic data were reported as follows in ppm (δ) from the internal standard (TMS, 0.0 ppm): chemical shift (multiplicity, coupling constant in Hz, integration). The ¹³C NMR spectra were referenced with the 77.16 resonance of CDCl₃.

Thermal properties were analyzed by DSC and TGA. Crystallization point and melting point were determined by using TA Instruments

Differential Scanning Calorimeter (DSC) Q1000 under N₂ atmosphere. Thermograms were recorded during heating from -50 °C to 100 °C scans at a heating rate of 10 °C min⁻¹ after cooling to -50 °C scans at a cooling rate of 10 °C min⁻¹. Thermal decomposition temperature was recorded by using TA Instruments SDT Q600 under Ar atmosphere. Heating rate and terminal temperature were set at 10 °C min⁻¹ and 500 °C, respectively.

Viscosity measurements were carried out on a Brookfield DV-II+cone/plate viscometer. Ionic conductivity was determined using a TOA-DKK CM-30R benchtop conductivity meter. The values of viscosity and ionic conductivity were measured three times, and averaged. Elemental analysis was performed on a US/CHNS-932.

Linear sweep voltammetry was performed with a CHI660A electrochemical workstation for the electrochemical stability window measurement at a scan rate of 10 mV s⁻¹ with a glassy carbon electrode (7.07×10^{-2} cm²) as a working electrode. The working electrode was polished before every measurement. A lithium electrode was used as both a counter electrode and a reference electrode. Note that the cut-off density of current was fixed at 1 mA cm⁻² according to the previous literature.

The lithium transference number was determined by a dc polarization combined with impedance spectroscopy following the technique

proposed by Bruce et al.¹⁶ The method consists of applying a small dc pulse to a symmetrical Li/electrolyte/Li cell and measuring the initial (I_0) and the steady-state (I_{ss}) current that flow through the cell. The cell was also monitored by impedance spectroscopy to measure the initial (R_0) and the final (R_{ss}) resistance of the two Li interfaces. Under these circumstances, the lithium transference number, t_{Li^+} , is given by

$$t_{Li^+} = I_{ss}(\Delta V - R_0 I_0) / I_0(\Delta V - R_{ss} I_{ss}) \quad (1)$$

Method A¹⁷ of flammability tests was performed with a Kovea TKT-9607 gas torch by directly exposing the flame of a gas torch to each binary electrolyte on a petri dish. After exposure, the flame was removed and each electrolyte on a petri dish was taken a picture after 10 and 20 seconds later. The flame-retarding properties of the binary electrolytes were evaluated by measuring the self extinguishing time (SET) normalized by the liquid mass.

Method B¹⁸ of flammability test was that glass fiber matrixes (2 cm x 4 cm) soaked with electrolytes were exposed to the flame of a candle for 3 seconds. After that, the flame was removed and the burning time of the glass fiber matrix was measured.

The surface morphology of the cycled $LiFePO_4$ cathode was observed by scanning electron microscope (SEM) on a Quanta 3D FEG (FEI)

after the 50th charge-discharge cycle.

2. General Procedure for the Preparation of the Pyrrolinium-based Ionic Liquids

2.1. General procedure for the preparation of *N*-alkyl-2-pyrrolidinone

To a tetrahydrofuran (THF, 200 mL) solution of sodium hydroxide (1.5 eq., 150.0 mmol) in a 250 mL RB flask was added 2-pyrrolidinone (100.0 mmol) and alkyl bromide (1.5 eq., 150.0 mmol) at room temperature. The reaction mixture was stirred at reflux condition for 24-48 hours. After the reaction was completed, the THF in the resulting solution was removed under reduced pressure. To remove the unreacted sodium hydroxide and other impurity, methylene chloride (200 mL) was added to the residue and the solution locate at -5 °C until the solid was crystallized. Afterward, the solid was removed by filtration and methylene chloride solution was followed by removing the solvent under reduced pressure afforded crude *N*-alkyl-2-pyrrolidinone. The residue was purified by column chromatography on SiO₂ with a solvent mixture (methylene chloride / methanol = 10 / 1) to give *N*-alkyl-2-

pyrrolidinone as a colorless oil.

***N*-propyl-2-pyrrolidone**

¹H NMR (400 MHz): δ 0.90 (t, *J* = 7.2, 3H), 1.54 (m, 2H), 2.02(m, 2H), 2.40 (t, *J* = 7.0, 2H), 3.24 (t, *J* = 7.2, 2H), 3.38 (t, *J* = 7.0, 2H). ¹³C NMR (100 MHz): δ 11.3, 18.0, 20.6, 31.1, 44.2, 47.1, 174.9. Anal. Calcd for C₇H₁₃NO: C, 66.10; H, 10.30; N, 11.01. Found: C, 66.43; H, 10.48; N, 11.31.

***N*-allyl-2-pyrrolidone**

¹H NMR (400 MHz): δ 2.02 (m, 2H), 2.41 (t, *J* = 7.2, 2H), 3.35 (t, *J* = 7.2, 2H), 3.89 (d, *J* = 6.0, 2H), 5.16 (m, 2H), 5.72 (m, 2H). ¹³C NMR (100 MHz): δ 17.8, 31.0, 45.2, 46.7, 117.8, 132.5, 174.7 Anal. Calcd for C₇H₁₁NO: C, 67.17; H, 8.86; N, 11.19. Found: C, 67.43; H, 8.94; N, 11.47.

2.2. General procedure for the preparation of *N*-alkyl-2-methoxypyrrolinium methylsulfates.

N-alkyl-2-pyrrolidinone (50 mmol) and dimethyl sulfate (55 mmol, 1.1 equiv) were added to a 100 mL RB flask at room temperature under nitrogen atmosphere. The reaction mixture was stirred at room temperature for 12 h. After the reaction was finished, the resulting

solution was washed successively with diethyl ether (50 mL \times 3) and ethyl acetate (50 mL \times 3) to remove the unreacted starting material. After the washed solution (bottom layer) was diluted with dichloromethane (50 mL), the resulting solution was dried over MgSO₄, filtered, and concentrated under reduced pressure to afford *N*-alkyl-2-methoxypyrrolinium methyl sulfate as a colorless oil.

***N*-ethyl-2-methoxypyrrolinium methyl sulfate (E(OMe)PyrI-MeSO₄)**

¹H NMR (400 MHz): δ 1.32 (t, J = 7.4, 3H), 2.44 (m, 2H), 3.37 (t, J = 7.9, 2H), 3.66 (q, J = 7.4, 2H), 3.74 (s, 3H), 4.00 (t, J = 7.9, 2H), 4.38 (s, 3H). ¹³C NMR (100 MHz): δ 11.2, 17.1, 29.5, 41.2, 51.9, 54.4, 62.6, 180.3. Anal. Calcd for C₈H₁₇NO₅S: C, 40.15; H, 7.16; N, 5.85; S, 13.40. Found: C, 40.09; H, 7.08; N, 5.77; S, 13.61.

***N*-propyl-2-methoxypyrrolinium methyl sulfate (P(OMe)PyrI-MeSO₄)**

¹H NMR (400 MHz): δ 0.97 (t, J = 7.5, 3H), 1.72 (m, 2H), 2.44 (m, 2H), 3.38 (t, J = 7.9, 2H), 3.55 (t, J = 7.5, 2H), 3.72 (s, 3H), 3.99 (t, J = 7.9, 2H), 4.38 (s, 3H). ¹³C NMR (100 MHz): δ 11.2, 17.4, 19.6, 29.7, 48.2, 52.7, 54.5, 62.8, 180.8. Anal. Calcd for C₉H₁₉NO₅S: C, 42.67; H, 7.56; N, 5.53; S, 12.66. Found: C, 42.91; H, 7.48; N, 5.43 ; S, 12.61.

***N*-allyl-2-methoxypyrrolinium methyl sulfate (A(OMe)PyrI-MeSO₄)**

^1H NMR (400 MHz): δ 2.43 (m, 2H), 3.39 (t, $J = 7.4$, 2H), 3.96 (t, $J = 7.4$, 2H), 4.21 (d, $J = 6.0$, 2H), 5.40 (m, 2H), 5.81 (m, 1H). ^{13}C NMR (100 MHz): δ 17.2, 29.6, 48.5, 52.2, 54.5, 62.8, 121.7, 128.2, 180.8. Anal. Calcd for $\text{C}_9\text{H}_{17}\text{NO}_5\text{S}$: C, 43.01; H, 6.82; N, 5.57; S, 12.76. Found: C, 42.91; H, 7.08; N, 5.77; S, 12.64.

2.3. General procedure for the anion metathesis - Preparation of *N*-alkyl-2-methoxypyrrolinium bis(fluorosulfonyl)imides.

To an aqueous solution of *N*-alkyl-2-methoxypyrrolinium methyl sulfate (20 mmol in 100 mL of distilled water) in a 250 mL RB flask was added lithium bis(fluorosulfonyl)imide (LiFSI) (1.1 equiv, 22 mmol) at room temperature. After the reaction mixture was stirred for 1 h, the bottom layer containing the desired product was partitioned from the top aqueous layer. The aqueous layer was extracted with CH_2Cl_2 (100 mL \times 2), and the combined organic layers together with the bottom layer were washed with distilled water (150 mL \times 3) again. Afterward, the washed organic layers were dried over MgSO_4 , filtered, and concentrated under reduced pressure to give a colorless oil of *N*-alkyl-2-methoxypyrrolinium bis(fluorosulfonyl)-imide as a colorless oil.

***N*-ethyl-2-methoxypyrrolinium bis(fluorosulfonyl)imide**
(E(OMe)PyrI-FSI)

¹H NMR (400 MHz): δ 1.31 (t, *J* = 7.5, 3H), 2.42 (m, 2H), 3.23 (t, *J* = 7.9, 2H), 3.62 (q, *J* = 7.5, 2H), 3.95 (t, *J* = 7.9, 2H), 4.32 (s, 3H). ¹³C NMR (100 MHz): δ 11.1, 16.9, 29.3, 41.5, 51.9, 62.7, 179.7. Anal. Calcd for C₇H₁₄N₂O₅S₂F₂: C, 27.27; H, 4.58; N, 9.09; S, 20.80. Found: C, 27.15; H, 4.55; N, 9.05; S, 20.98.

***N*-propyl-2-methoxypyrrolinium bis(fluorosulfonyl)imide**
(P(OMe)PyrI-FSI)

¹H NMR (400 MHz): δ 0.97 (t, *J* = 7.5, 3H), 1.70 (m, 2H), 2.40 (m, 2H), 3.23 (t, *J* = 7.9, 2H), 3.49 (q, *J* = 7.5, 2H), 3.94 (t, *J* = 7.9, 2H), 4.31 (s, 3H). ¹³C NMR (100 MHz): δ 11.1, 17.0, 19.5, 29.2, 48.1, 52.7, 62.7, 180.2. Anal. Calcd for C₈H₁₆N₂O₅S₂F₂: C, 29.81; H, 5.00; N, 8.69; S, 19.89. Found: C, 29.87; H, 5.11; N, 8.72; S, 19.97.

***N*-allyl-2-methoxypyrrolinium bis(fluorosulfonyl)imide**
(A(OMe)PyrI-FSI)

¹H NMR (400 MHz): δ 2.39 (m, 2H), 3.24 (t, *J* = 8.0, 2H), 3.89 (t, *J* = 8.0, 2H), 4.15 (t, *J* = 6.0, 2H), 4.33 (s, 3H), 5.41 (m, 2H), 5.75 (m, 1H). ¹³C NMR (100 MHz): δ 17.0, 29.4, 48.9, 52.3, 63.0, 122.9, 127.4, 180.3. Anal. Calcd for C₈H₁₄N₂O₅S₂F₂: C, 30.00; H, 4.41; N, 8.75; S, 20.02. Found: C, 29.98; H, 4.37; N, 8.77; S, 19.97.

2.4. Preparation of the binary electrolytes of E(OMe)Pyrl-FSI

To measure the viscosity, ionic conductivity, lithium ion transference number, and electrochemical performance, the ionic liquids were mixed with the 1.0 M LiTFSI as a lithium salt. Then, the mixtures were stirred for 10 min at room temperature and dried at 55 °C in vacuum oven for 8 hours for removing the water in ILs. It should be noted that we selected lithium bis(trifluoromethanesulfonyl)imide (LiTFSI) instead of LiFSI as a lithium salt for the electrolyte solution, because (1) LiTFSI has a similar chemical structure to LiFSI (compatibility with FSI-based ILs), (2) it is more resistive to the corrosion of a current collector,¹³ and (3) it is cheaper than LiFSI and commercially available. The commercial carbonate (EC/EMC = 3/7 with 1.0 M LiPF₆) was measured to compare the physical and electrochemical properties of the ionic liquids.

3. Electrochemical Performance

3.1. Preparation of electrode and cell fabrication

LiFePO₄ powder that is provided by EIG company was used as an

active material, and size of particles 100-500 nm by observation with SEM. For preparation of the composite electrode, LiFePO_4 powder and super-P conductive additive were dispersed in the binder solution, which are prepared by dissolving of polyvinylidene fluoride (PVdF) in *N*-methyl-2-pyrrolidinone (NMP). Electrode composition of the active material, super-P and the binder was 8:1:1 by weight. The resulting slurry was coated on a piece of Al foil as current collector and dried in a vacuum oven at 120 °C. After drying process, the electrode sheet was punching in a disk shape with diameter 1.2 cm and LiFePO_4 loading was 1.05 mg cm^{-2} . Li/LiFePO₄ half-cells (2032 coin-type) were fabricated to characterize the electrode performance with prepared electrolytes. To this end, the LiFePO_4 composite electrode was loaded into the coin cells along with Li foil. The glass fiber filter (Advantec, GA-55, 0.21 mm thick, 0.6 μm pore) was used as separator. To investigate the effect of the prepared electrolytes, 1.0 M lithium salt concentration was fixed in each prepared electrolytes.

3.2. Electrochemical characterization

The galvanostatic charge (de-lithiation) and discharge (lithiation) cycling of Li/LiFePO₄ cells were conducted using a WBCS3000 cycler at 25, 50 and 60 °C in a constant current mode. Pre-cycling step was

added in order to obtain full activation of LiFePO_4 . To this end, the galvanostatic charge-discharge processes are two methods; 1) the cycling of $\text{Li}/\text{LiFePO}_4$ cells with different electrolytes were 50 cycles with 0.1 C-rate as the current density (1 C-rate is 150 mAh g^{-1}), 2) to investigate the rate capability, the charge and discharge current of $\text{Li}/\text{LiFePO}_4$ cells were varied by evaluating current density from 0.1 C to 5 C (0.1 C \rightarrow 0.2 C \rightarrow 0.5 C \rightarrow 1 C \rightarrow 2 C \rightarrow 5 C), when the cycling is recorded by 3 cycles, respectively. The voltage range was 2.5 – 3.9 V (vs Li/Li^+).

References

1. K. Xu, *Chem. Rev.* 114 (2014) 11503–11618
2. (a) V. Etacheri, R. Marom, R. Elazari, G. Salitra, D. Aurbach, *Energy Environ. Sci.* 4 (2011) 3243–3262. (b) L. Lu, X. Han, J. Li, J. Hu, M. Ouyang, *J. Power Sources* 226 (2013) 272-288.
3. (a) C.M. Julien, A. Mauger, K. Zaghbi, H. Groult, *Inorganics* 2 (2014) 132–154. (b) J.W. Fergus, *J. Power Sources* 195 (2010) 939–954. (c) J. Chen, *Materials* 6 (2013) 156–183.
4. J.S. Wilkes, M.J. Zaworotko, *J. Chem. Soc., Chem. Commun.* (1992) 965-967.
5. (a) G. Min, T. Yim, H.Y. Lee, D.H. Huh, E. Lee, J. Mun, S.M. Oh, Y.G. Kim, *Bull. Korean Chem. Soc.* 27 (2006) 847–852. (b) G. Min, T. Yim, H.Y. Lee, H. Kim, J. Mun, S. Kim, S.M. Oh, Y.G. Kim, *Bull. Korean Chem. Soc.* 28 (2007) 1562–1566. (c) T. Yim, C.Y. Choi, J. Mun, S.M. Oh, Y.G. Kim, *Molecules* 14 (2009) 1840–1851. (d) H. Kim, J. Kang, J. Mun, S.M. Oh, T. Yim, Y.G. Kim, *ACS Sustainable Chem. Eng.* 4 (2016) 497-505.
6. (a) V.L. Boulaire, R. Grée, *Chem. Commun.* (2000) 2195-2196 (b) N.M. Henze *Synlett.* (1996) 1091-1092. (c) K.M. Hillenkemp, *Anal. Chem.* 60 (1998) 2299-2301.
7. F. Zhou, Y. Liang, W. Liu, *Chem. Soc. Rev.* 38 (2009) 2590–2599

8. (a) S. Fang, Y. Jin, L. Yang, S. Hirano, K. Tachibana, S. Katayama, *Electrochim. Acta* 56 (2011) 4663-4671. (b) Y. Jin, S. Fang, M. Chai, L. Yang, K. Tachibana, S. Hirano, *J. Power Sources* 226 (2013) 210-218. (c) S. Fang, Z. Zhang, Y. Jin, L. Yang, S. Hirano, K. Tachibana, S. Katayama, *J. Power Sources* 196 (2011) 5637-5644. (d) Y. Jin, J. Zhang, J. Song, Z. Zhang, S. Fang, L. Yang, S. Hirano, *J. Power Sources* 254 (2014) 137-147.
9. H. Matsumoto, H. Sakaebe, K. Tatsumi, M. Kikuta, E. Ishiko, M. Kono, *J. Power Sources* 160 (2006) 1308–1313.
10. (a) J.C. Dearden, *Sci. Total Environ.* 109-110 (1991) 59-68. (b) R.J.C. Brown, R.F.C. Brown, *J. Chem. Educ.* 77 (2000) 724-731. (c) P. Bonhôte, A.P. Dias, N. Papageorgiou, K. Kalyanasundaram, M. Grätzel, *Inorg. Chem.* 35 (1996) 1168-1178.
11. (a) Z.B. Zhou, H. Matsumoto, K. Tatsumi, *Chem. Eur. J.* 10 (2004) 6581-6591. (b) Z.B. Zhou, H. Matsumoto, K. Tatsumi, *Chem. Eur. J.* 11 (2005) 752-766. (c) Z.B. Zhou, H. Matsumoto, K. Tatsumi, *Chem. Eur. J.* 12 (2006) 2196-2212. (d) S.H. Fang, L. Yang, J.X. Wang, M.T. Li, K. Tachibana, K. Kamijima, *Electrochim. Acta* 54 (2009) 4269-4273.
12. (a) G.H. Lane, *Electrochim. Acta* 83 (2012) 513–528. (b) A. Budi, A. Basile, G. Opletal, A.F. Hollenkamp, A.S. Best, R.J. Rees, A.I. Bhatt, A.P. O’Mullane, S.P. Russo, *J. Phys. Chem. C* 116 (2012)

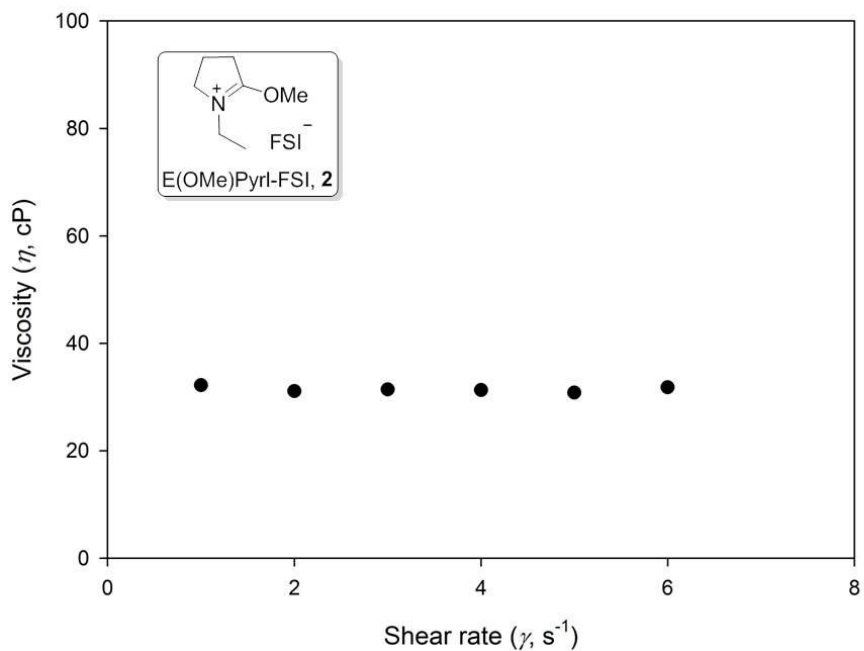
- 19789–19797. (c) L. Xiao, K.E. Johnson, *J. Electrochem. Soc.* 150 (2003) E307–E311.
13. (a) K. Park, S. Yu, C. Lee, H. Lee, *J. Power Sources* 296 (2015) 197–203. (b) M. Kerner, N. Plylahan, J. Scheers, P. Johansson, *Phys. Chem. Chem. Phys.* 17 (2015) 19569–19581. (c) E. Cho, J. Mun, O.B. Chae, O.M. Kwon, H. Kim, J.H. Ryu, Y.G. Kim, S.M. Oh, *Electrochem. Commun.* 22 (2012) 1–3. (d) L. Zhang, L. Chai, L. Zhang, M. Shen, X. Zhang, Y.S. Battaglia, T. Stephenson, H. Zheng, *Electrochim. Acta* 127 (2014) 39–44. (e) T. Evans, J. Olson, V. Bhat, S. Lee, *J. Power Sources* 269 (2014) 616–620.
14. (a) R.A. DiLeo, A.C. Marschilok, K.J. Takeuchi, E.S. Takeuchi, *J. Electrochem. Soc.* 160 (2013) A1399–A1405. (b) E.T. Fox, E. Paillard, O. Borodin, W.A. Henderson, *J. Phys. Chem. C* 117 (2013) 78–84. (c) M.S. Ding, K. Xu, S.S. Zhang, K. Amine, G.L. Henriksen, T.R. Jow, *J. Electrochem. Soc.* 148 (2001) A1196–A1204. (d) H.P. Chen, J.W. Fergus, B.Z. Jang, *J. Electrochem. Soc.* 147 (2000) 399–406.
15. H. Yoon, P.C. Howlett, A.S. Best, M. Forsyth, D.R. MacFarlane, *J. Electrochem. Soc.* 160 (2013) A1629–A1637
16. P.G. Bruce, J. Evans, C.A. Vincent, *Solid State Ionics* 28-30 (1988) 918–922.
17. (a) L. Lombardo, S. Brutti, M.A. Navarra, S. Panero, P. Reale, *J.*

Power Sources 227 (2013) 8–14. (b) I. Quinzeni, S. Ferrari, E. Quartarone, C. Tomasi, M. Fagnoni, P. Mustarelli, J. Power Sources 237 (2013) 204–209. (c) H. Li, J. Pang, Y. Yin, W. Zhuang, H. Wang, C. Zhai, S. Lu, RSC Adv. 3 (2013) 13907–13914.

18. C. Arbizzani, G. Gabrielli, M. Mastragostino, J. Power Sources 196 (2011) 4801–4805.

APPENDICES

Study of Pyrrolinium-based ILs as Newtonian or non-Newtonian fluid

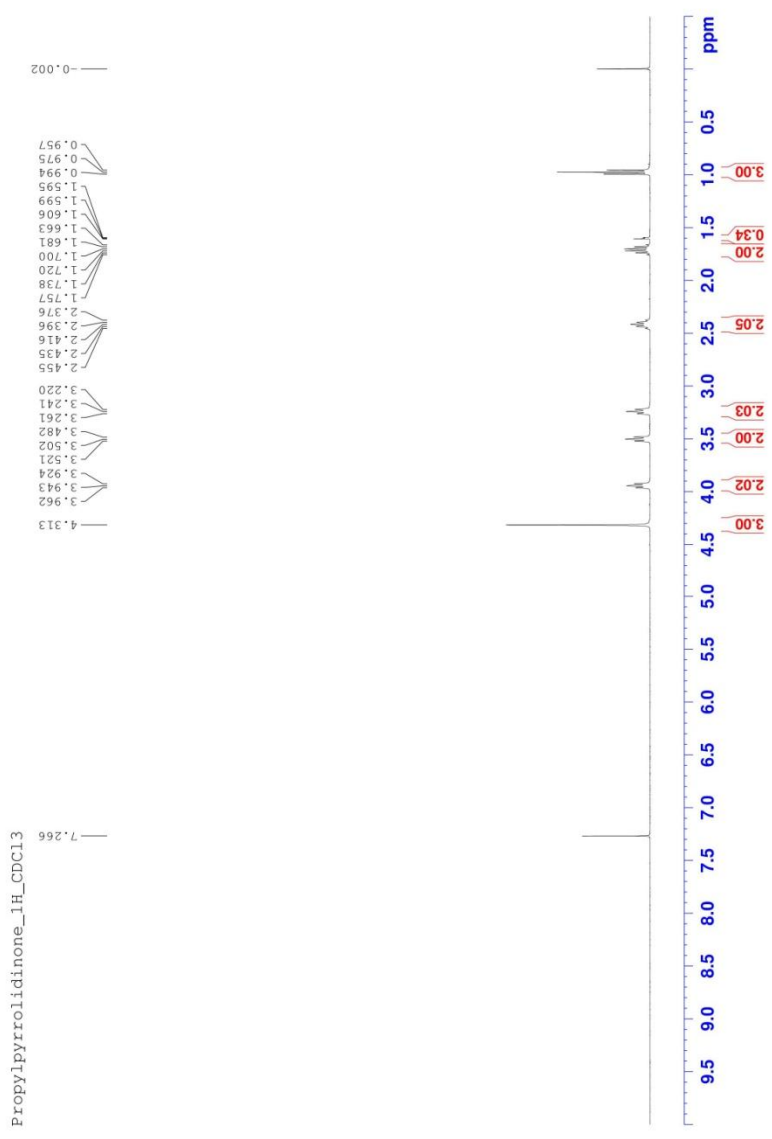


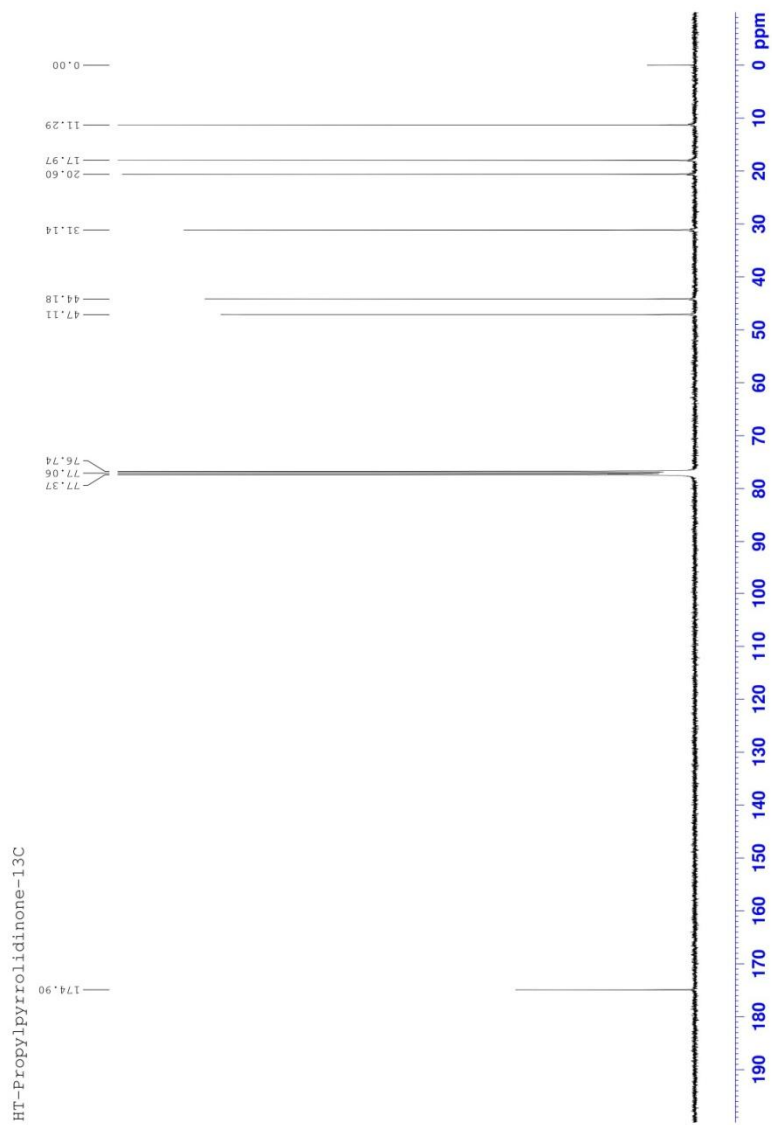
Shear rate (γ , s^{-1})	Viscosity (η , cP)
1	32.2
2	31.1
3	31.4
4	31.3
5	30.8
6	31.8

List of ^1H NMR and ^{13}C NMR Spectra of

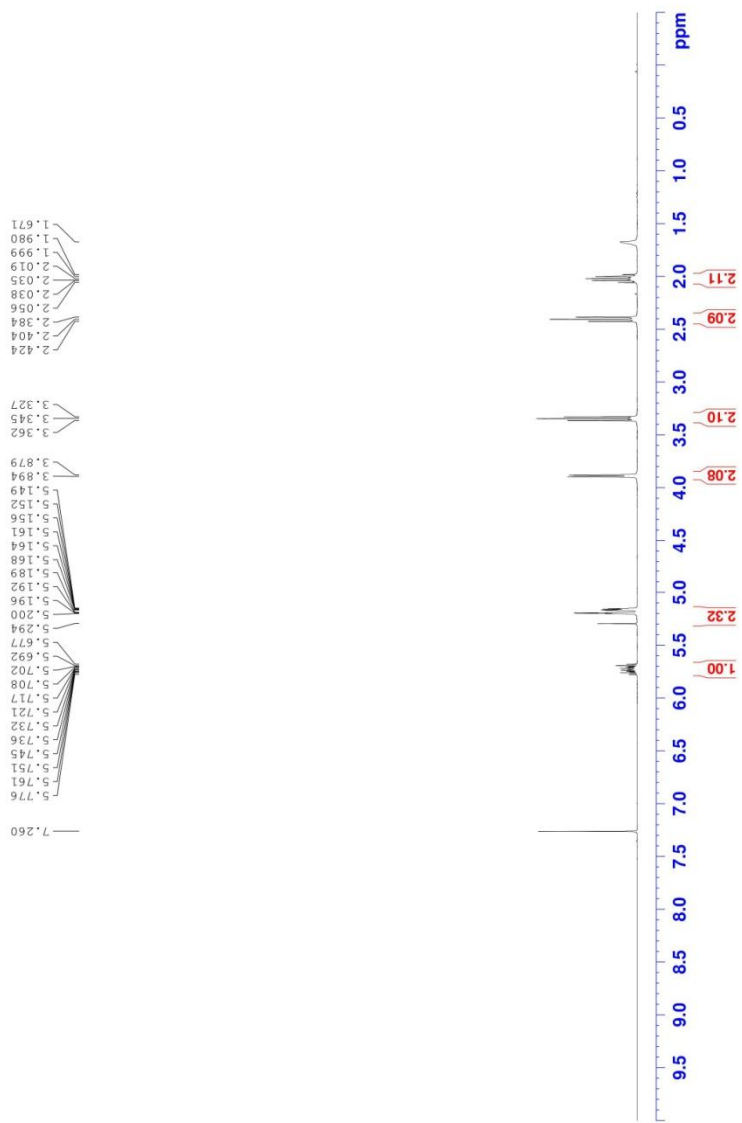
N-alkyl-2-pyrrolidinone

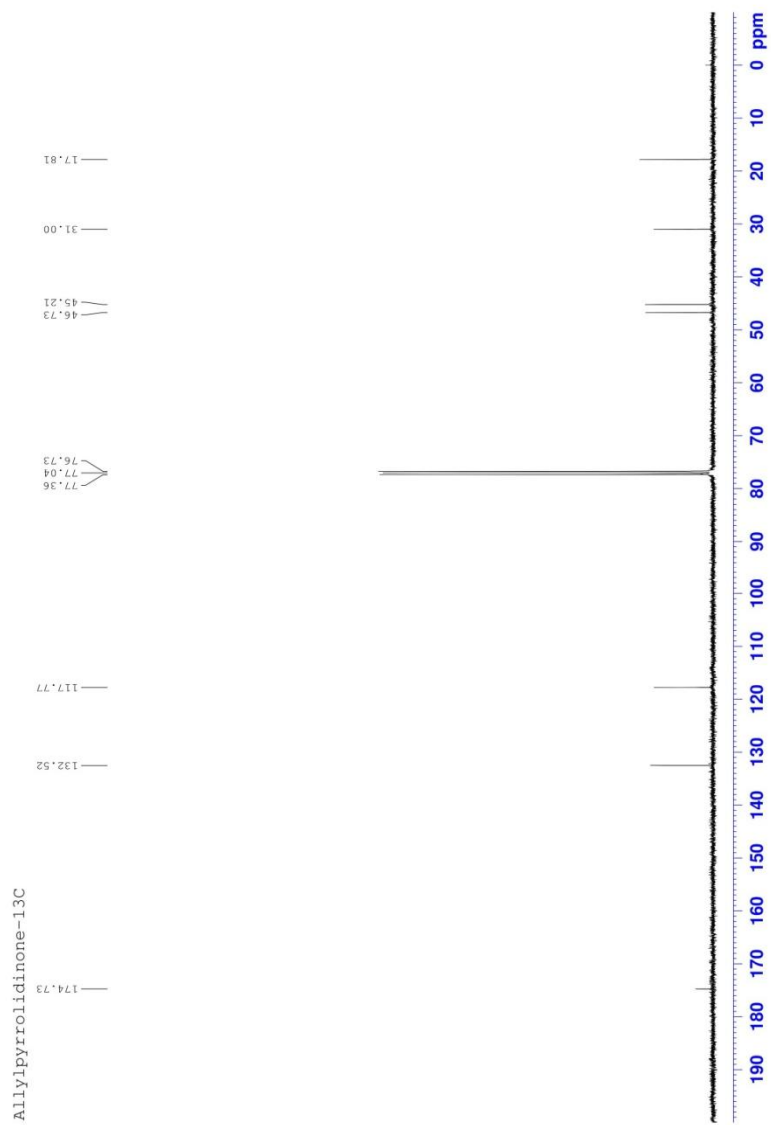
1. 400 MHz ^1H NMR Spectrum (chloroform-*d*) of *N*-propyl-2-pyrrolidinone.....87
2. 100 MHz ^{13}C NMR Spectrum (chloroform-*d*) of *N*-propyl-2-pyrrolidinone88
3. 400 MHz ^1H NMR Spectrum (chloroform-*d*) of *N*-allyl-2-pyrrolidinone89
4. 100 MHz ^{13}C NMR Spectrum (chloroform-*d*) *N*-allyl-2-pyrrolidinone90





Allylpyrrolidinone_1H_CDCl3



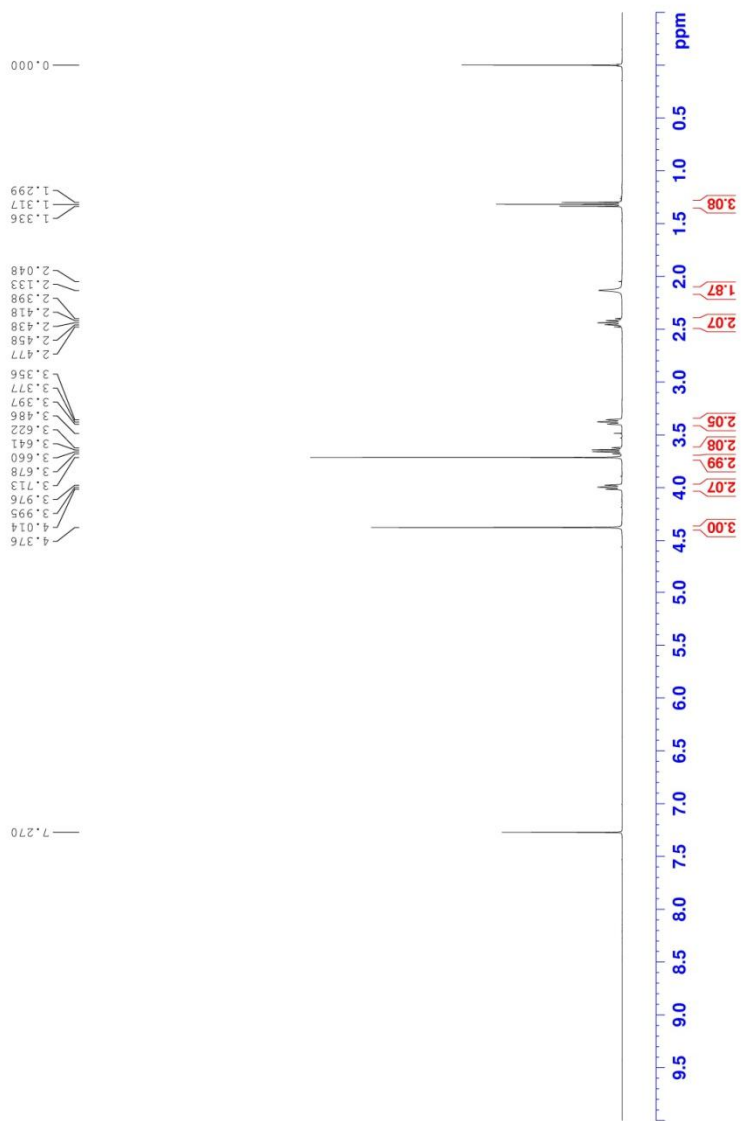


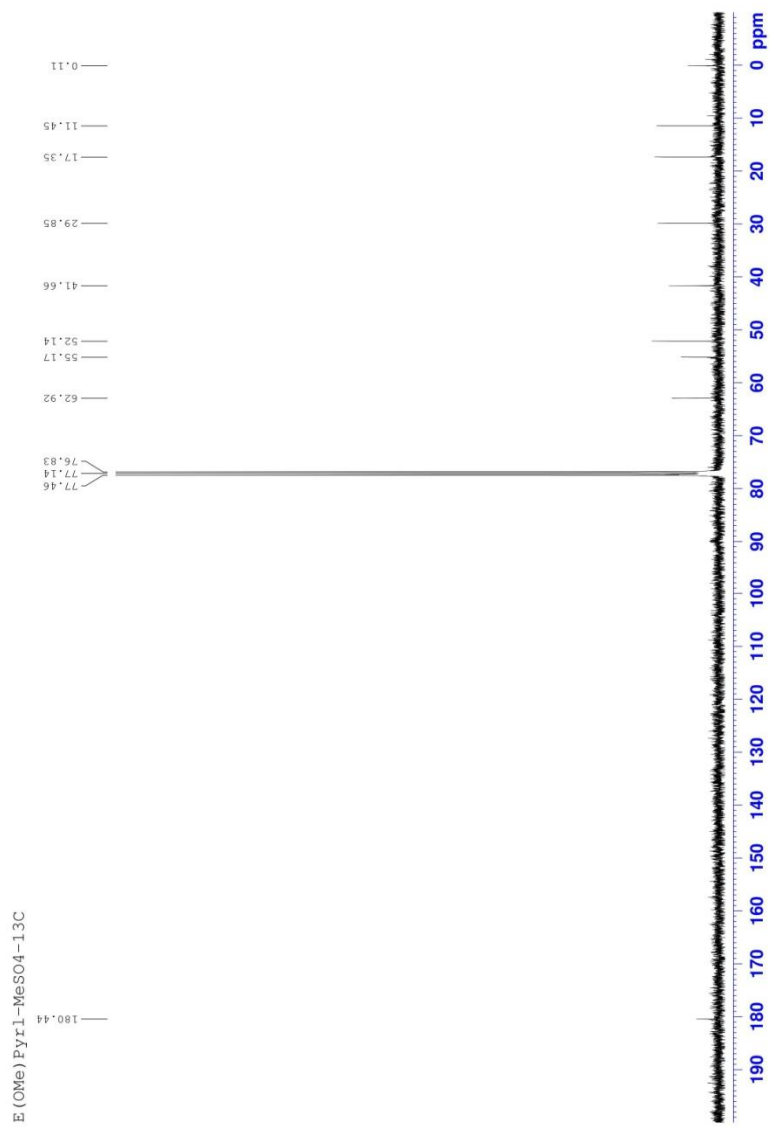
List of ^1H NMR and ^{13}C NMR Spectra of

N-alkyl-2-pyrrolidinone

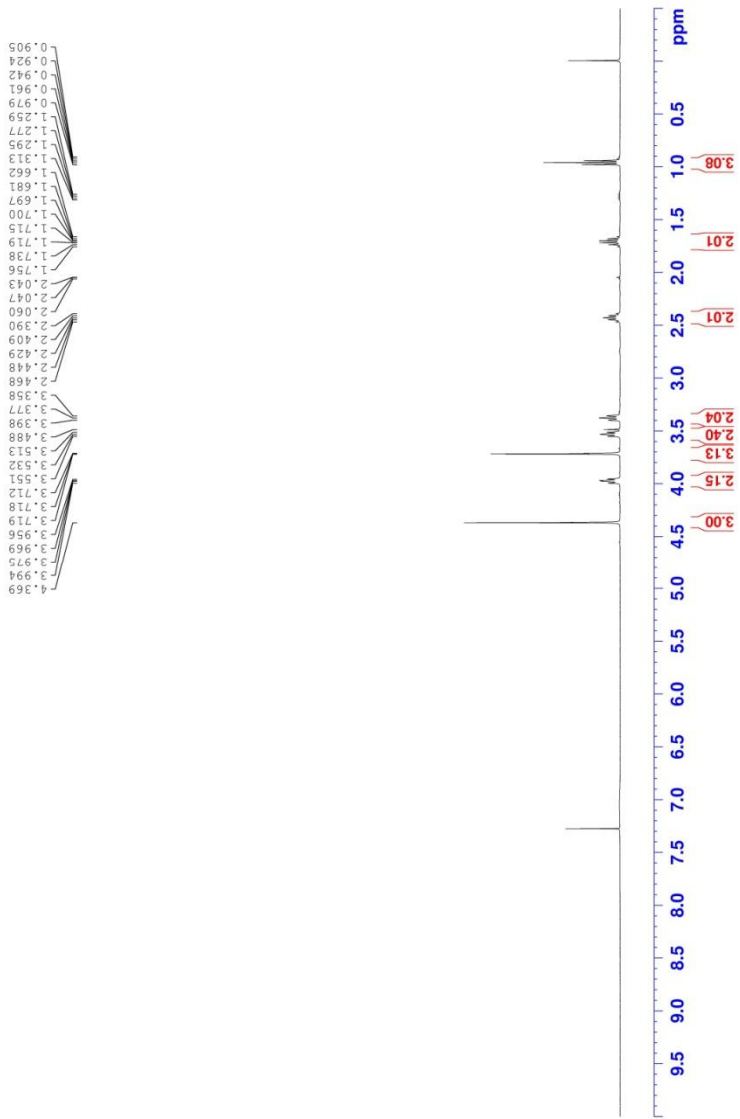
1. 400 MHz ^1H NMR Spectrum (chloroform- <i>d</i>) of Compound 2- MeSO ₄	92
2. 100 MHz ^{13}C NMR Spectrum (chloroform- <i>d</i>) of Compound 2- MeSO ₄	93
3. 400 MHz ^1H NMR Spectrum (chloroform- <i>d</i>) of Compound 3- MeSO ₄	94
4. 100 MHz ^{13}C NMR Spectrum (chloroform- <i>d</i>) Compound 3- MeSO ₄	95
5. 400 MHz ^1H NMR Spectrum (chloroform- <i>d</i>) of Compound 4- MeSO ₄	96
6. 100 MHz ^{13}C NMR Spectrum (chloroform- <i>d</i>) Compound 4- MeSO ₄	97

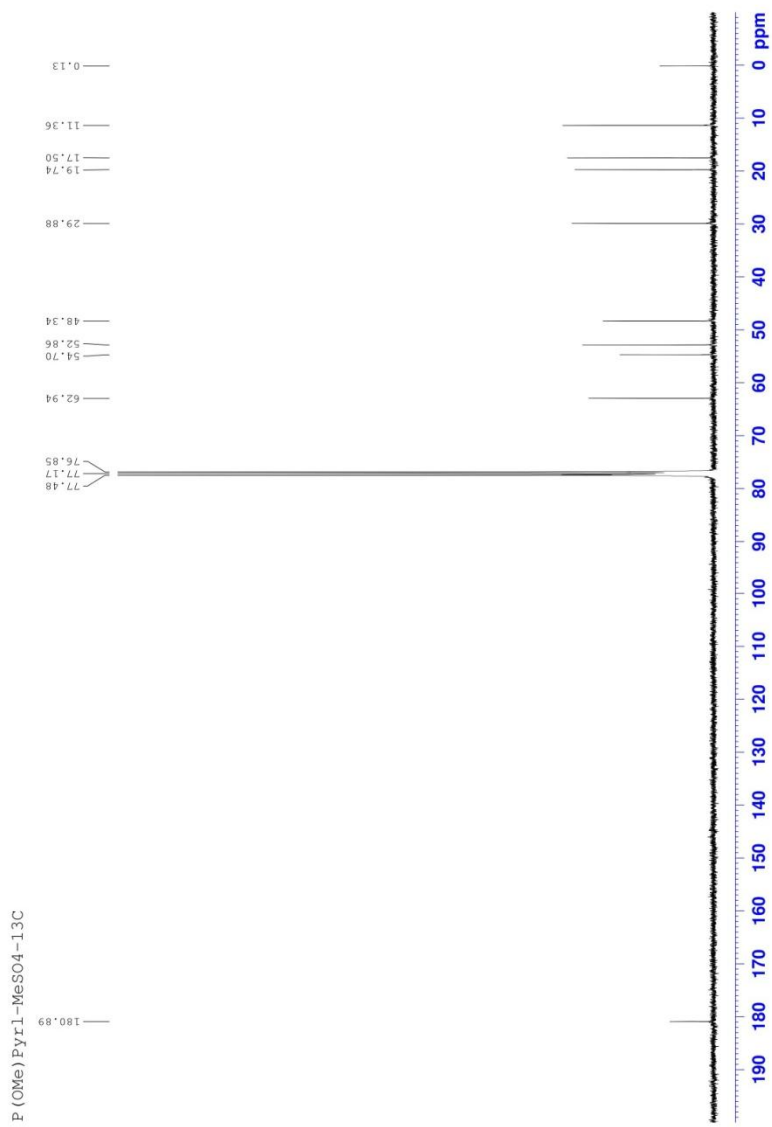
E (OMe) Pyr1-MeSO4

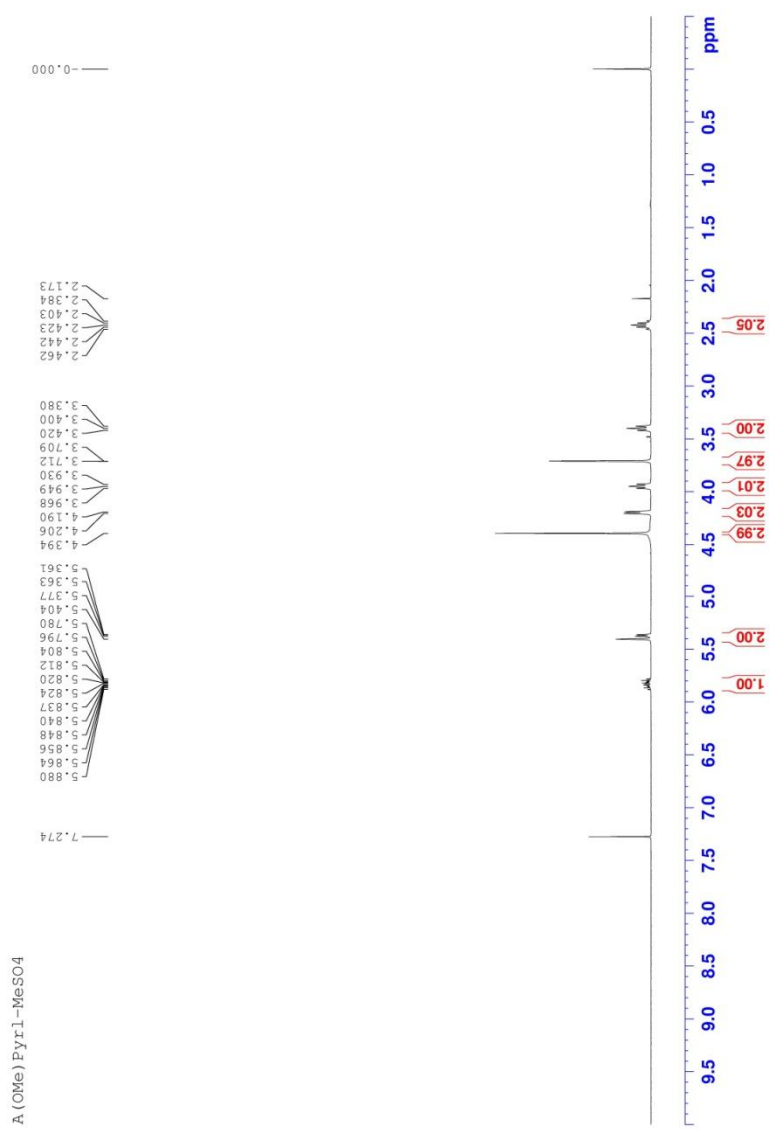


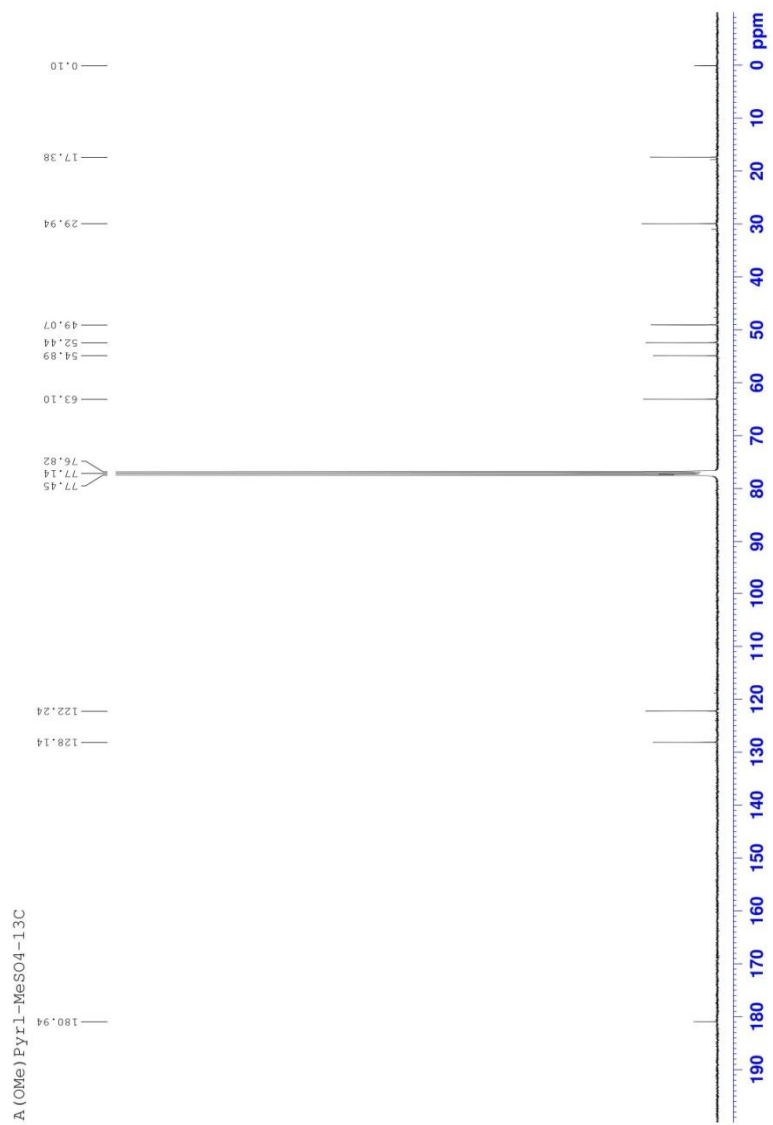


P (OMe) Pyr1-MeSO4





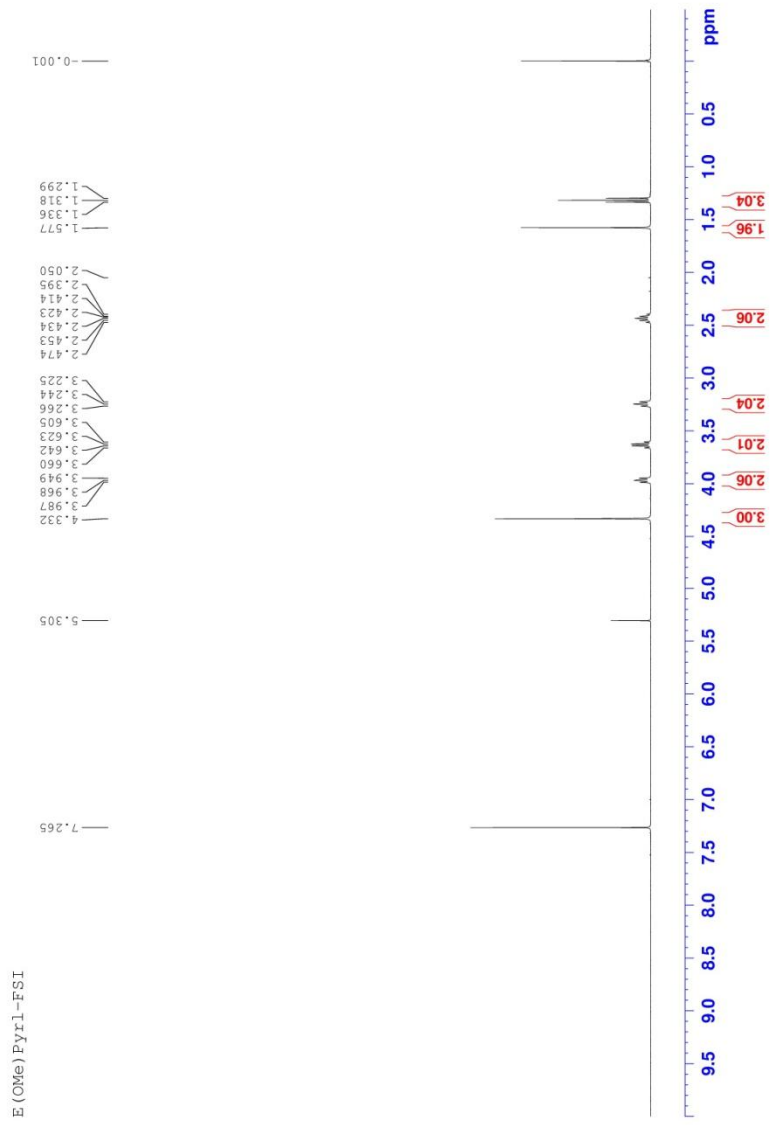


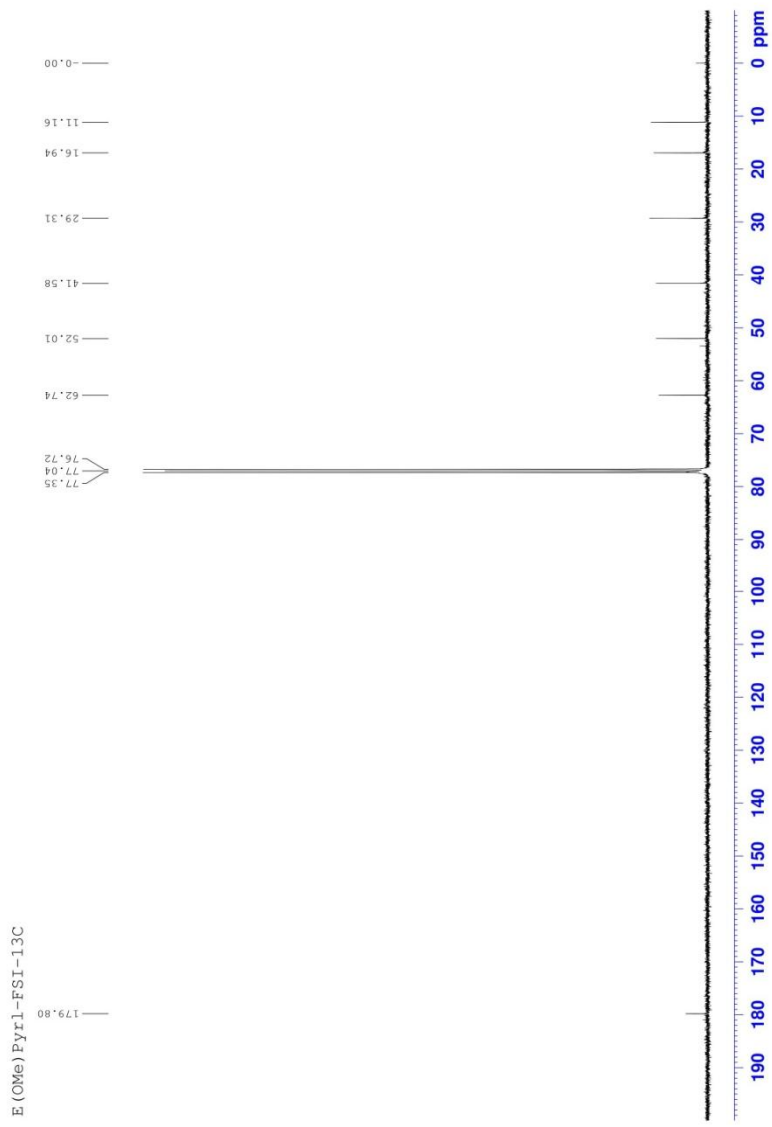


List of ^1H NMR and ^{13}C NMR Spectra of

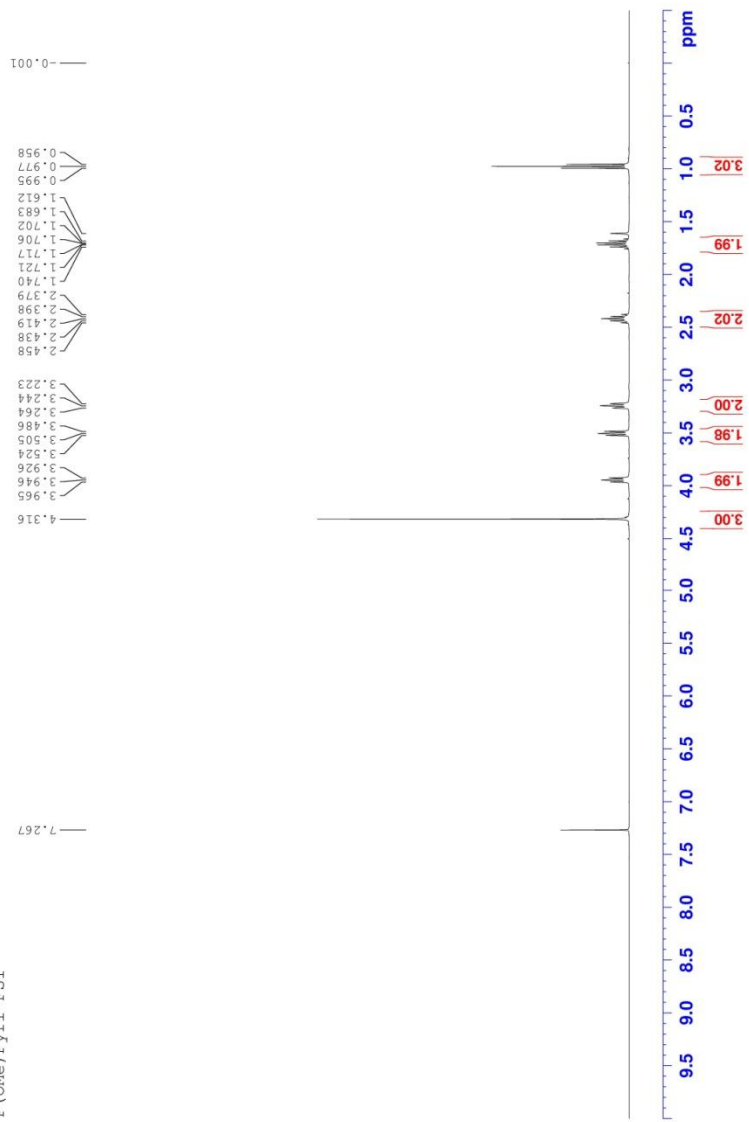
N-alkyl-2-pyrrolidinone

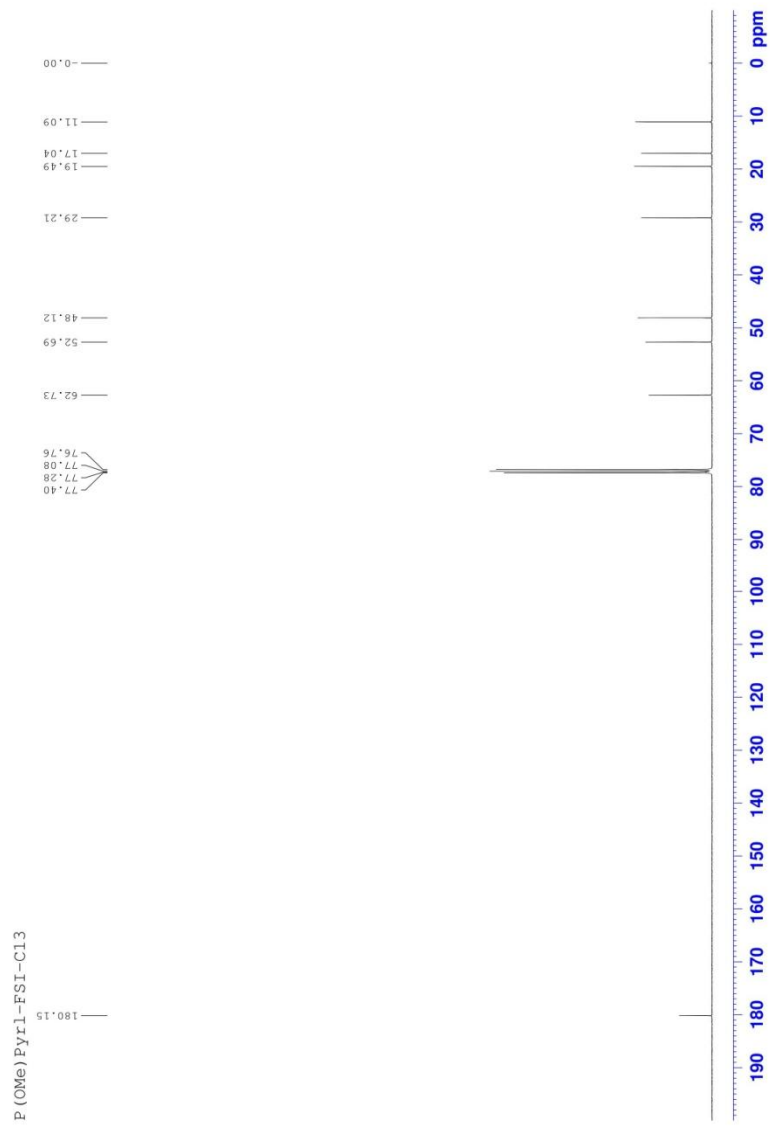
1. 400 MHz ^1H NMR Spectrum (chloroform- <i>d</i>) of Compound 2	99
2. 100 MHz ^{13}C NMR Spectrum (chloroform- <i>d</i>) of Compound 2	100
3. 400 MHz ^1H NMR Spectrum (chloroform- <i>d</i>) of Compound 3	101
4. 100 MHz ^{13}C NMR Spectrum (chloroform- <i>d</i>) Compound 3	102
5. 400 MHz ^1H NMR Spectrum (chloroform- <i>d</i>) of Compound 4	103
6. 100 MHz ^{13}C NMR Spectrum (chloroform- <i>d</i>) Compound 4	104



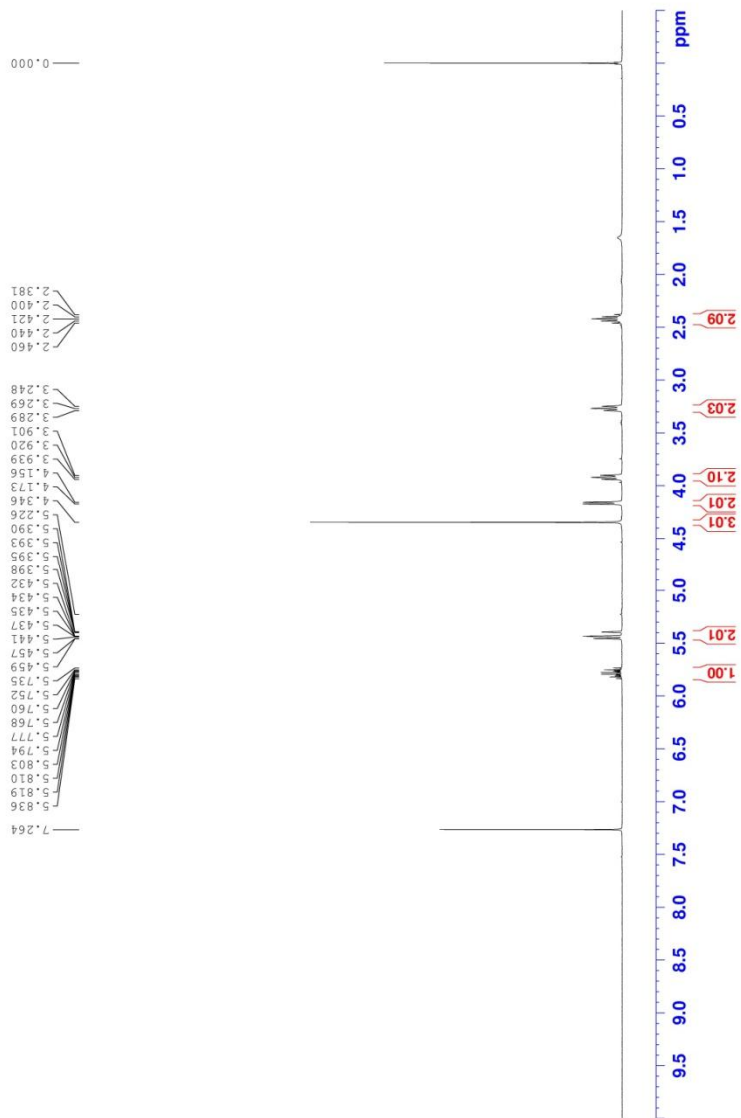


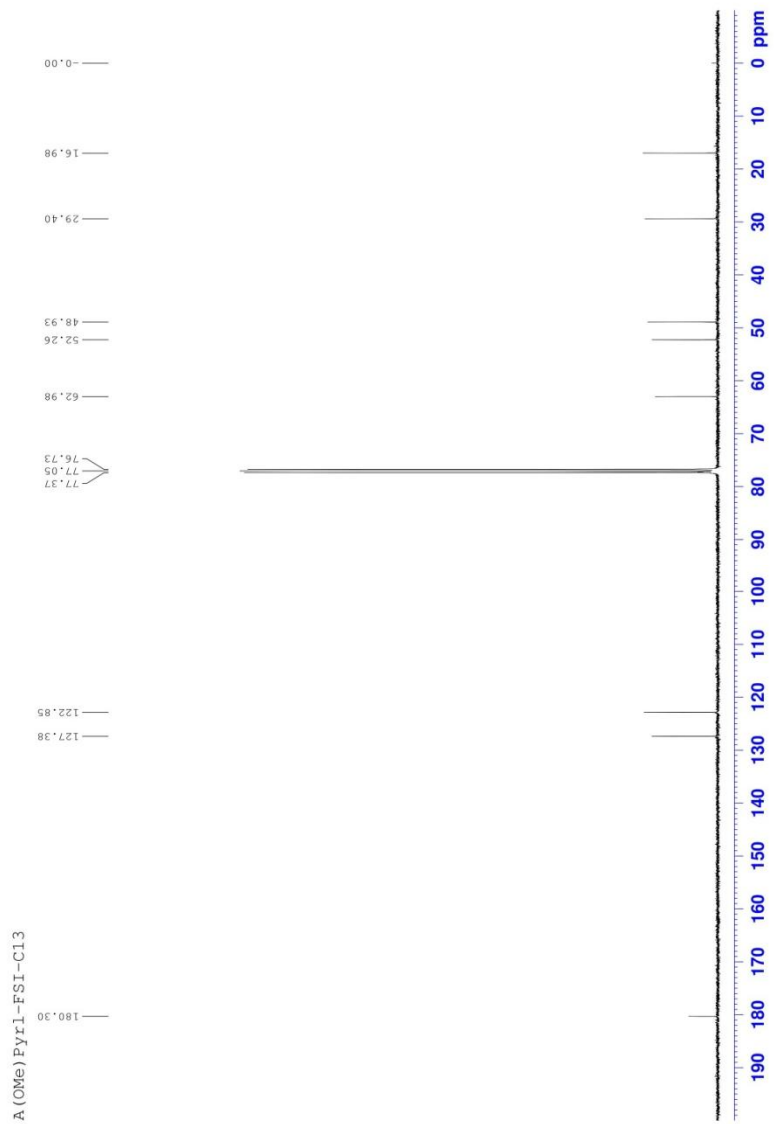
P (OMe) Pyr1-FSI





A (OMe)Pyr1-FSI





ABSTRACT IN KOREAN

초록

리튬 이차전지의 전해액으로 사용하기 위해, 다양한 합성전략이 들어간 이온성 액체를 합성 후 평가하였다. 기존의 이온성 액체 중 많이 알려져 있는 이미다졸륨계열의 물질들은 낮은 이온 전도도와 우수한 열적 안정성을 기반으로 많이 연구되었다. 하지만, 이미다졸륨에 존재하는 반응성이 뛰어난 수소로 인해 전기화학적으로 불안정하게 되었고 리튬 이온전지에 적용하는데 큰 어려움을 겪게 된다. 이를 해결하고자, 많은 연구자들은 다양한 방법을 시도하는데, 그 중에서 가장 성공적으로 연구된 것은 포화고리를 기반으로 하는 이온성 액체인 피롤리디늄 또는 피페리디늄 계열의 이온성 액체의 개발이다. 이중에서도 피롤리디늄은 오각형으로서 육각형인 피페리디늄보다 한 개 적은 탄소를 지니고 있으며, 이와 같은 영향으로 인해 점도가 매우 낮아지게 된다. 하지만 그럼에도 불구하고 피롤리디늄 계열의 이온성 액체는 상대적으로 높은 점도를 지니게 되는데 이를 해결하고자 다음과 같은 치환기 또는 반응기들을 도입하였다.

양이온의 구조들을 연구하는 과정에서, 산소 원자가 들어간 알콕시 치환체를 도입하고 더 평면적인 구조를 지니게 하기 위해 고리 내에 이중결합을 도입하고자 하였다. 이를 바탕으로 2-메톡시 피롤리늄 계열의 이온성 액체를 전략적으로 합성하였으며, 이와 함께 물과 산소에 내성이 있는 bis(fluorosulfonyl)imide (FSI)를 음이온으로 선택하였다. FSI 음이온은 기존에 알려진 bis(trifluoromethanesulfonyl)imide (TFSI)에 비해 더 낮은 점도, 높은 이온 전도도를 지니는 것으로 알려져 있다.

위와 같은 전략적 이온성 액체를 합성하였으며, 리튬 이온전지의 전해질로서 적합한지 확인하기 위해 다양한 물성들을 측정하였다. 피롤리늄 계열의 이온성 액체 중에서 에틸기가 치환된 *N*-ethyl-2-methoxypyrrrolinium FSI (E(OMe)Pyr1-FSI, **2**)가 가장 높은 이온 전도도 (13.0 mS cm^{-1})를 지녔으며, 전기화학적인 측면에서는 allyl기가 치환된 **4**번 물질이 가장 안정적인 성능을 나타냈다. 또한 피롤리늄 계열의 이온성 액체들은 모두 넓은 범위의 전위에서도 안정적인 구동을 하였는데, 이는 반응성이 뛰어난 수소를 제거했기에 가능하다고 판단한다.

위와 같은 결과들을 바탕으로 이온전도도가 가장 뛰어났던 2번 이온성 액체와 기존에 사용되는 카보네이트 혼합물을 다양한 비율로 혼합하여 리튬 이온전지의 전해질로서의 가능성을 확인하고자 하였다. 40 또는 60 질량비율의 이온성 액체를 혼합한 물질이 가장 좋은 이온전도도를 지녔으며 (16.2 mS cm^{-1} for E 40, 15.5 mS cm^{-1} for E 60 at $60 \text{ }^\circ\text{C}$), 특히 60 질량비율의 이온성 액체가 혼합된 물질은 발화지연제의 역할을 훌륭히 수행할 수 있음을 확인하였다. 이런 결과들을 바탕으로 전기화학적 안정성을 확인하였으며, 모든 혼합물들은 카보네이트와 비슷한 성능을 보여줬다.

이와 같은 연구를 통해서, 기존에 이온성 액체가 가지고 있는 높은 점도, 낮은 전도도, 전기화학적 불안정성을 해결함과 동시에 카보네이트 전해질이 가지고 있던 열적 불안정성을 해결하여 좀 더 열적 및 전기화학적 안정성을 지닌 리튬 이온전지에 한발 다가갈 수 있었다고 판단한다.

주요어 : 리튬이온전지, 피롤리논 계열의 이온성 액체, FSI 음이온, 열적 안정성, 혼합전해질

학번: 2009-20986